Journal of Biogeography (J. Biogeogr.) (2017)

ORIGINAL ARTICLE

Diversification in arid mountains: biogeography and cryptic diversity of *Pristurus rupestris rupestris* in Arabia

Joan Garcia-Porta[1#], Marc Simó-Riudalbas[1], Michael Robinson[2] and Salvador Carranza[1*]

[1]*Institute of Evolutionary Biology (CSIC-Universitat Pompeu Fabra), Passeig Marítim de la Barceloneta, 37-49, 08003 Barcelona, Spain,* [2]*Department of Biology, College of Science, Sultan Qaboos University, PO Box 36 Al-Khod Muscat, Oman*

*Correspondence: Salvador Carranza, Institute of Evolutionary Biology (CSIC-University Pompeu Fabra), Passeig Marítim de la Barceloneta, 37-49, 08003 Barcelona, Spain.
E-mail: salvador.carranza@ibe.upf-csic.es

#Present address: Center for Ecological Research and Forestry Applications (CREAF) Spanish National Research Council (CSIC) Campus of the Autonomous University of Barcelona, Cerdanyola del Vallès, 08193, Spain

ABSTRACT

Aim To understand the patterns of genetic, geographical and morphological diversification in the Arabian gecko subspecies *Pristurus rupestris rupestris*, and to discuss the various processes that generate and shape diversity in arid mountain ranges.

Location Hajar Mountains, south-eastern Arabian Peninsula.

Methods We sampled 466 individuals across the entire range of *P. r. rupestris* in the Hajar Mountains and sequenced one mitochondrial gene for all the samples, and one extra mitochondrial and four nuclear genes for a subset of 75 specimens. A total of 155 individuals were characterized morphologically. Multilocus coalescent-based methods were used for species delimitation, for phylogenetic inference of species trees and to investigate the diversification dynamics. Multivariate statistics were used to analyse morphological data.

Results Our molecular methods revealed 14 candidate species hidden within the subspecies *P. r. rupestris*. Diversification started *c.* 15 Ma, but most of the lineages have evolved in the last 7 Ma of the mountains' orogeny, producing a mosaic of allopatric taxa. Secondary interchange has occurred between high and low elevation lineages, and along the mountain chain between unrelated lineages formerly separated by mountain blocks. Morphological variation between the 14 candidate species is slight, but a high elevation robust morphotype is identified.

Main conclusions Our results support the notion that mountain ranges constitute important centres of diversification in arid regions, and also act as 'species pumps' into surrounding areas. We also demonstrate that arid mountains may constitute important reservoirs of cryptic diversity, even in common and widespread species. This, and previous evidence, suggest that the Hajar Mountains are a biological hotspot and an important reservoir of diversity. We therefore suggest that these mountains should be a priority focal point for conservation in Arabia.

Keywords
allopatry, Arabia, arid mountains, biodiversity, biogeography, cryptic species, diversification, evolution, systematics

INTRODUCTION

Mountain regions are great reservoirs of diversity, containing half of the currently defined biodiversity hotspots (Kohler & Maselli, 2012). This is because they offer great opportunities for adaptive and non-adaptive diversification. From an adaptive standpoint, mountains have strong environmental gradients that can lead to ecological speciation (Fuchs *et al.*, 2011). From a non-adaptive (or not necessarily adaptive) perspective, allopatric or peripatric speciation may occur in mountains by isolation of populations as continuous species ranges are fragmented during mountain orogenies, interrupting gene flow (Vuilleumier & Monasterio, 1986; Randi *et al.*, 2000; Antonelli *et al.*, 2009; Schweizer *et al.*, 2011).

© 2017 John Wiley & Sons Ltd

Journal of Biogeography

Such processes have an important role in arid regions, where low rainfall and plant productivity do not provide much room for high levels of diversity and diversification (Wiens *et al.*, 2013). In such extreme environments, mountain ranges potentially act as important pumps of regional biodiversity.

This study focuses on one of such mountain ranges, the Hajar Mountains, a long mountain range that borders the Arabian Sea and the Gulf of Oman in the south-eastern Arabian Peninsula (Fig. 1). These mountains are topographically complex consisting of three distinct divisions separated by lowlands, and reaching over 3000 m at Jebel Shams, in the central mountain block (Fig. 1). The highest elevations contain grassland, shrubs and an open juniper-olive tree woodland. Four distinct vegetative zones occur from *c.* 500 m to the highest summit (Ghazanfar, 1991). Their isolation, climatic diversity and complex structure make the Hajars one of the most biotically diverse regions of southern Arabia, with numerous endemic plants and animals (e.g. Arnold & Gallagher, 1977; Ghazanfar, 1991; Brinkmann *et al.*, 2009; Carranza & Arnold, 2012; Carranza *et al.*, 2016; de Pous *et al.*, 2016).

One of the most conspicuous reptiles is the small sphaerodactylid gecko *Pristurus rupestris* Blanford, 1874. Because of its abundance and broad distribution its current conservation status is of 'Least Concern' (IUCN, 2016). *Pristurus rupestris* is characterized by being mostly diurnal, heliothermic and, like other species of the genus, individuals signal each other by waving their tails (Arnold, 1993, 2009; Badiane *et al.*, 2014). A recent taxonomic revision restricted the range of *P. rupestris* to the Hajar Mountains (subspecies *P. r. rupestris*) and some coastal areas of western Iran (subspecies *P. r. iranicus*) (Badiane *et al.*, 2014; Yousofi *et al.*, 2015).

Despite having a very broad distribution and probably being the most abundant reptile in southern Arabia, the populations of *P. r. rupestris* from the Hajar Mountains have always been considered as a single, morphologically uniform subspecies (Arnold & Gallagher, 1977; Arnold, 1980, 1986, 1993, 2009). However, many recent studies have revealed the existence of cryptic species complexes in common and widespread species

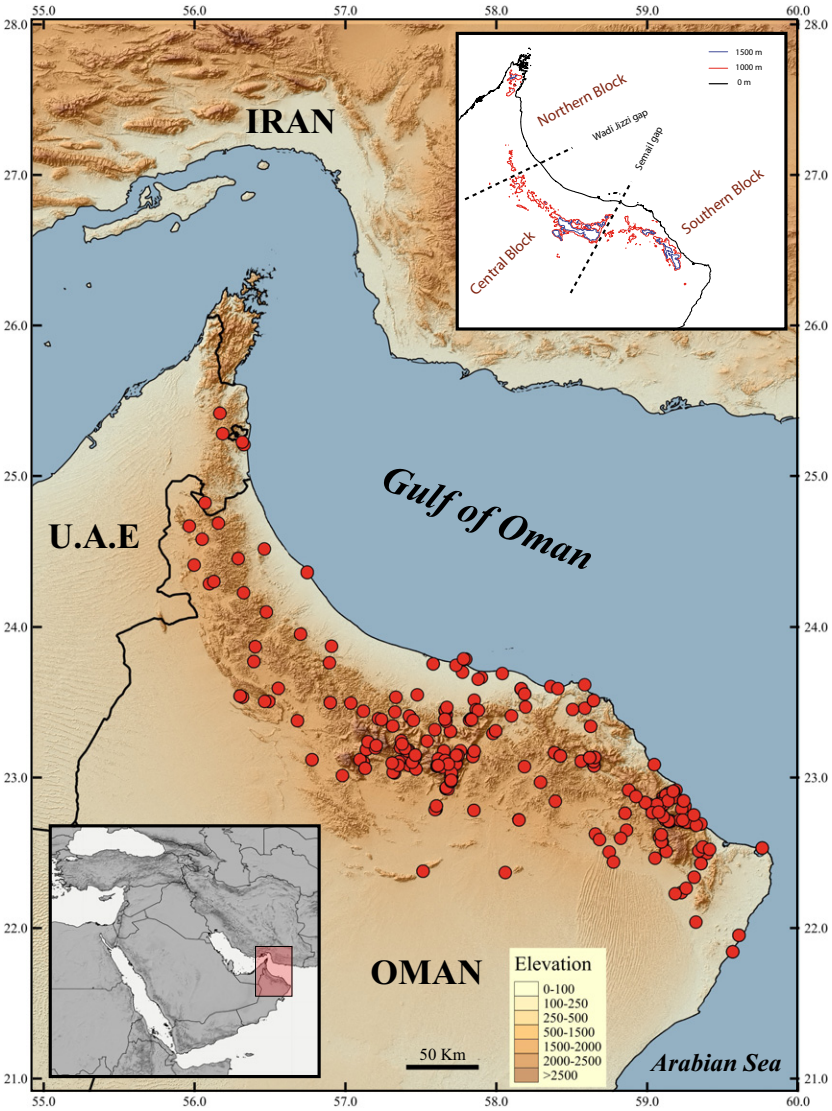

Figure 1 Map of the Hajar Mountains of south-eastern Arabia and sampling locations of *Pristurus rupestris rupestris*. The upper right plot depicts the topographic complexity of the Hajar Mountains with topographic discontinuities that dissect the range into northern, central and southern blocks, physically separated by the Wadi Jizzi and Semail gaps.

© 2017 John Wiley & Sons Ltd

in arid mountain ranges, including the Hajar Mountains (Busais & Joger, 2011; Pepper *et al.*, 2011; Barata *et al.*, 2012a, b; Carranza & Arnold, 2012; Brito *et al.*, 2014; Metallinou *et al.*, 2015; Šmíd *et al.*, 2015; Carranza *et al.*, 2016; de Pous *et al.*, 2016), and previous preliminary studies suggested that *P. r. rupestris* could be no exception (Badiane *et al.*, 2014).

In this study we aim to explore three main questions: (1) How much genetic and phenotypic diversity exists within *P. r. rupestris*? (2) Is the phylogenetic structure and genetic divergences within *P. r. rupestris* consistent with the existence of multiple species? (3) What is the role of the Hajar Mountains in producing this phylogenetic structure?

MATERIALS AND METHODS

Sampling

Eight field campaigns were carried out between 2005 and 2014 to explore the diversity of the reptiles in Oman, including the endemic fauna from the Hajar Mountains. Numerous collections were made along the 650 km length of the mountains and the adjacent lowlands, covering the entire distribution range of *P. r. rupestris*. We selected 466 tissue samples from 233 different localities and 155 vouchers to assess the genetic and phenotypic structure of *P. r. rupestris*. Figure 1 illustrates the distribution of the sampling localities, and information on the specimens included in the molecular and morphological analyses is provided in Table S1.

Molecular analyses

Four molecular data sets were assembled for the phylogenetic, phylogeographical and species delimitation analyses. Details of the laboratory, phylogenetic and species delimitation protocols and analyses are in the Supporting Information (see Appendix S1).

Identification and delimitation of mitochondrial lineages

To obtain a first estimation of the genetic diversity within *P. r. rupestris*, the *12S* mitochondrial gene was amplified and sequenced for 466 samples. After removing identical sequences, we aligned the remaining unique 221 sequences (data set 1) with MAFFT 7 (Katoh & Toh, 2008) and produced an ultrametric tree and a set of 250 post-burn-in trees using BEAST 1.8.0 (Drummond & Rambaut, 2007). We then objectively identified and delimited deep mitochondrial lineages with the general mixed Yule-coalescent model (GMYC) (Pons *et al.*, 2006; Fujisawa & Barraclough, 2013). Using the summary tree, this model was implemented in a maximum likelihood and Bayesian framework (using the 250 post-burn trees), by means of the packages' 'splits' (Ezard *et al.*, 2009) and 'bGMYC' (Reid & Carstens, 2012), respectively, both available in R (R 3.1.0, R Development Core Team, 2014).

Multilocus coalescent-based species delimitation

From the 16 lineages defined by GMYC (see Results), we amplified and sequenced the mitochondrial *cytb* and the nuclear *c-mos*, *rag1*, *rag2* and *mc1r* genes for a subset of specimens and assembled data set 2. This data set included 2,459 bp from 75 specimens, including at least four specimens from each GMYC lineage (except lineage 16, from which only a single specimen could be amplified for the nuclear genes; see Table S1). The four nuclear loci were used to test whether the mitochondrial lineages defined by the GMYC model were also supported by nuclear data. We assessed this using a coalescent-based species delimitation approach in the program Bayesian Phylogenetics and Phylogeography (BP&P) 2.2 (Yang & Rannala, 2010; see also Olave *et al.*, 2014). To obtain the best tree for the analysis containing all 16 lineages defined by the GMYC model, we used *BEAST 1.8.0 to calculate a species tree (guide tree; see Fig. S2) from data set 2. We ran BP&P analyses with the four nuclear genes (*c-mos, rag1, rag2*, and *mc1r*), which allowed us to evaluate the GMYC lineage delimitation hypothesis with loci not used to generate it. We ran six different types of analyses, each one having a different combination of prior settings and rjMCMC algorithms. After confirming convergence and good mixing in each analysis we evaluated the posterior probabilities (pp) of all cladogenetic events recovered in our guide tree. We only considered as candidate species those that presented high support values across all different runs (pp > 0.95).

Dating the radiation of *P. r. rupestris*

To date the onset of diversification within *P. r. rupestris*, we assembled data set 3 by placing one representative from each of the 14 candidate species delimited by BP&P (see Results) in the phylogenetic context of a wide representation of all species of geckos available in GenBank. Working at this large phylogenetic scale allowed using five calibration points scattered across the phylogeny of Gekkota, all external to our group of interest. Data set 3 consisted of up to 1614 bp of the mitochondrial *12S* and *cytb* and the nuclear *c-mos, rag1* and *rag2* genes for one representative of each of the 14 candidate species of *P. r. rupestris* plus 435 species downloaded from GenBank, including representatives of 117 of the 123 recognized gecko genera (see Table S2; Uetz *et al.*, 2016). Phylogenetic analysis and divergence times were estimated in BEAST 1.8.0 using methods and calibration points specified in the electronic supplementary material.

Inference of a calibrated coalescent-based species tree for the *P. r. rupestris* radiation

A species tree of the 14 candidate species of *P. r. rupestris*, was estimated with data set 2 (see above) using *BEAST (Heled & Drummond, 2010). To obtain the species tree in units of time, we imported into our *BEAST analysis the

© 2017 John Wiley & Sons Ltd

substitution rates for *12S*, *c-mos*, *rag1* and *rag2* genes and the age of the root of the *P. r. rupestris* radiation obtained from the BEAST analysis of data set 3 (see above).

Genetic distances

Uncorrected genetic distances (*P*-distances) of the *12S* mitochondrial gene for the 14 candidate species were inferred from data set 1 with MEGA 7.0 (Kumar *et al.*, 2016).

Geographical structure

We used three different approaches to understand the geographical structure within *P. r. rupestris*. First, to infer the phylogeographical history and reconstruct the ancestral origin of *P. r. rupestris* in the Hajar Mountains we used the Bayesian stochastic search variable selection (BSSVS; Lemey *et al.*, 2009) of the discrete phylogeographical model as implemented in BEAST 1.8.0. To maximize geographical representation we used data set 4, which included all 466 sequences of *12S* with the tree topology of the main lineages constrained to match the *BEAST tree topology obtained from the analysis of data set 2 (see Fig. S2). We established the phylogeographical traits according to three discrete topographic discontinuities of the Hajar Mountains, the northern, central and southern blocks, which are physically separated by the Wadi Jizzi and Semail gaps (Fig. 1). Models, prior settings and parameters were the same used for the BEAST analysis of data set 1 (see the electronic supplementary material). Secondly, to assess if diversification had occurred along altitudinal gradients (Kozak & Wiens, 2007; Cadena *et al.*, 2012), we compared the mean altitudes and ranges of the candidate species in a phylogenetic framework by mapping their means onto the phylogeny. To approximate altitudinal change through time, we used the function 'phenogram' of the R package 'phytools' (Revell, 2012) to reconstruct ancestral altitudes. Finally, we evaluated the degree of range overlap between candidate species by creating a 100 m buffer around each one of the 233 unique localities with QGIS 2.6.1 and checking the number of different candidate species coexisting within each buffered locality. The 100 m buffer was selected because the Hajar Mountains can have dramatic altitudinal and topographic changes within a few hundred metres (Mandaville, 1977).

Morphological differentiation

We characterized the morphology of each candidate species with 11 different measurements. Body size was measured from the snout to the cloaca (snout-vent length = SVL); head shape was defined by the length from the snout to the auricular opening (HL), by the maximum width (HW) and by the maximum depth (HD). Body proportions were quantified by the axilla to groin distance (AGL) and by the body width at the level of the scapular and pelvic girdles (ASG and APG respectively). Forelimb proportions included measurements of the length of the brachium (BL), length of the antebrachium (AL) and hindlimb proportions of the thigh (TL) and crus lengths (CL). Tail length was not measured because most of the specimens had regenerated tails. All measurements were taken three times by the same person using a digital calliper (± 0.1 mm). To improve normality and homoscedasticity, data were $\log_{10}$-transformed and the means were used in the analysis.

A total of 155 specimens (all adults) were measured, with a minimum of two, a maximum of 24 and a mean of 11 specimens per candidate species (see Table S3). To remove the effect of body size on the shape variables, we computed their residuals against SVL. We tested for sex differences in SVL and in each of the shape measurements (using the residuals) by fitting linear models using each body measurement as dependent variable and sex as the independent variable (using the package 'stats'). The morphospace occupied by each candidate species was determined by a Principal Component Analysis (PCA; package 'ade4'; Dray & Dufour, 2007). To assess whether size and shape differences existed between the candidate species, we conducted a permutational ANOVA on body size (using the package 'stats') and a permutational multivariate ANOVA (perMANOVA) on the first eight PC axes of shape variation (using the R package 'vegan' Oksanen *et al.*, 2013). Finally, a linear discriminate function analysis with all $\log_{10}$-transformed measurements was used to determine if specimens could be correctly assigned to the candidate species identified by molecular data, with the R package 'MASS' (Venables & Ripley, 2002).

RESULTS

Identification and delimitation of mitochondrial lineages and multilocus coalescent-based species delimitation

Pristurus rupestris rupestris is extensively distributed in the Hajar Mountains and adjacent lowlands, with the exception of the northern region above 25°25′ N latitude, where not a single specimen was found (Fig. 1). The results of the GMYC and bGMYC analyses supported 16 different mitochondrial lineages (see Fig. S1). The coalescent-based species delimitation analyses (BP&P) produced different results depending on the prior settings and rjMCMC algorithms, giving low support values for some of the splits between the deep mitochondrial lineages (see Fig. S2). The topological placement of the splits having low support varied depending on the prior parameterization: when big population sizes were combined with deep divergence times, the nodes separating lineages 4 and 5, and 10 and 11 received low support (pp < 0.93). However, when big population sizes were combined with shallow divergences times, or when small population sizes were combined with shallow divergences times, only the split separating lineages 10 and 11 had low support (pp < 0.80). Consequently, we conservatively collapsed the mitochondrial lineages 4 and 5 and 10 and 11 into putative species 4.5 and 10.11, respectively.

© 2017 John Wiley & Sons Ltd

Genetic distances for the *12S* mitochondrial gene between all 14 candidate species resulting from the BP&P analysis were very high in most comparisons (5–20%), with the only exception of sister species 1 and 2 (2.9%), and 6 and 7, (2.8%), which present moderate levels of genetic divergence (see Table S4).

Dating the radiation of *P. r. rupestris*

The topology of the phylogeny inferred with data set 3 including the 14 candidate species detected in *P. r. rupestris*, plus 435 additional species of geckos was generally consistent with previously published phylogenies of Gekkota (Gamble *et al.*, 2008, 2011, 2012; Pyron *et al.*, 2013), with 62% of the nodes having pp support values > 0.90 (see Fig. S3). According to our estimates, the age of the crown radiation of Gekkota occurred around 96.6 Ma [95% high posterior density interval (HPD), 65–114 Ma], which is in the range of most estimates from previous studies (Vidal & Hedges, 2005; Hugall *et al.*, 2007; Gamble *et al.*, 2008; Jones *et al.*, 2013; Garcia-Porta *et al.*, 2016). The onset of diversification in the genus *Pristurus* began *c.* 37 (HPD 30–47) Ma and in *P. r. rupestris* began at *c.* 16 (HPD 10–22) Ma. Remarkably, divergence times within *P. r. rupestris* are similar to those between other species of *Pristurus* and to other species of geckos, independently supporting the deep structure found within this 'subspecies' (see Fig. S3).

Inference of a calibrated coalescent-based species tree for the *P. r. rupestris* radiation

The species tree of the *P. r. rupestris* species complex produced with *BEAST (Fig. 2) is consistent with the phylogenetic relationships of this radiation recovered in the large phylogenetic tree that includes most gecko genera (see Fig. S3). The species tree revealed four highly supported clades whose detailed distribution ranges are shown in Fig. S4. Clade 1 (candidate species 8 and 9) is mostly limited to lowland areas of the southern block, clade 2 (candidate species 6 and 7) is endemic to high elevations in the southern block, clade 3 (candidate species 10.11, 12, 13, 14 and 15) is distributed throughout the whole region, including the southern, central and northern blocks, and clade 4 (candidate species 1, 2, 3 and 4.5) is mainly distributed in the central and southern blocks. Finally, candidate species 16, is an isolated lineage from the southern block, and is associated with low support to clade 4 in both *BEAST and BEAST analyses of data sets 2 and 3 respectively (Fig. 2 and see Fig. S3).

Geographical structure

The results of the discrete phylogeographical analysis carried out with data set 4 using the BSSVS model are presented in Fig. 3a (see also Fig. S5) and suggest that diversification likely started in the southern block (68%, 76%, 74% and 65% of probability in the four deepest nodes of the phylogenetic tree; from deepest to shallowest). Diversification in clades 1, 2 and 3 also started in the southern block (92%, 99% and 73% of probability respectively) with some specimens within clade 1 (candidate species 9), and several specimens within clade 3 (all specimens from candidate species 14 and most specimens of candidate species 10.11) having colonized the central block from the southern block. Moreover, within candidate species 10.11 there are some individuals that apparently have recently colonized the northern block from the central block (91% of probabilit). The origin of clade 4 is inferred to have been in the central block (62% of probability), where candidate species 1, 2 and 4.5 are currently distributed. Candidate species 3 colonized the southern block from the central block (63% of probability) and very recently it has back colonized the central block (93% of probability).

Range overlap between candidate species within the 100 m buffer zone is uncommon, occurring in only 12 of the 233 localities (see Table S5). The great majority of the candidate species have disjunct distributions (94.9%), consistent with a prevalent situation of allopatry in this species complex (Rivas, 1964; Barraclough & Vogler, 2000). Moreover, all sympatric localities had a maximum of two candidate species: only one case included two sister candidate species (6 and 7) and the remaining 11 sympatric localities had pairs of candidate species from different clades (see Table S5).

Morphological differentiation

Morphological differentiation was negligible between sexes and therefore we pooled all sexes together in all posterior analyses (results not shown). Our analyses detected some morphological differentiation among candidate species. The permutational ANOVA on body size was significant (P-value < 0.00001) showing some size variation despite of the high levels of size overlap observed among species (Fig. 4). The perMANOVA analysis of the first eight components of the PCA (explaining 96% of the shape variance) identified significant differences among several candidate species (P-value < 0.00001). The PCA analysis of body shape concluded that most species overlap extensively in their morphologies (Fig. 4), but candidate species 6, 7, 14 have more robust phenotypes, with wider and deeper heads, wider scapular and pelvic girdles (PC1), shorter extremities (PC2) and shorter axilla-groin lengths (PC3) (see Table S6). The position of candidate species 16 in the PCA is uncertain because only two specimens were included in the analysis (see Table S3). All three taxa with robust phenotypes live at higher altitudes according to our elevational reconstructions (Fig. 3b). However, the linear discriminate function analysis failed to assign individual specimens to their respective candidate species in more than 70% of the comparisons (mean correct assignment 26%) (see Table S7). Robust phenotypes of candidate species 6, 7 and 14 were assigned to other robust phenotypes in 64%, 90% and 80% of the comparisons, respectively, and correctly assigned to their respective candidate species in 40% of the comparisons. Although the

© 2017 John Wiley & Sons Ltd

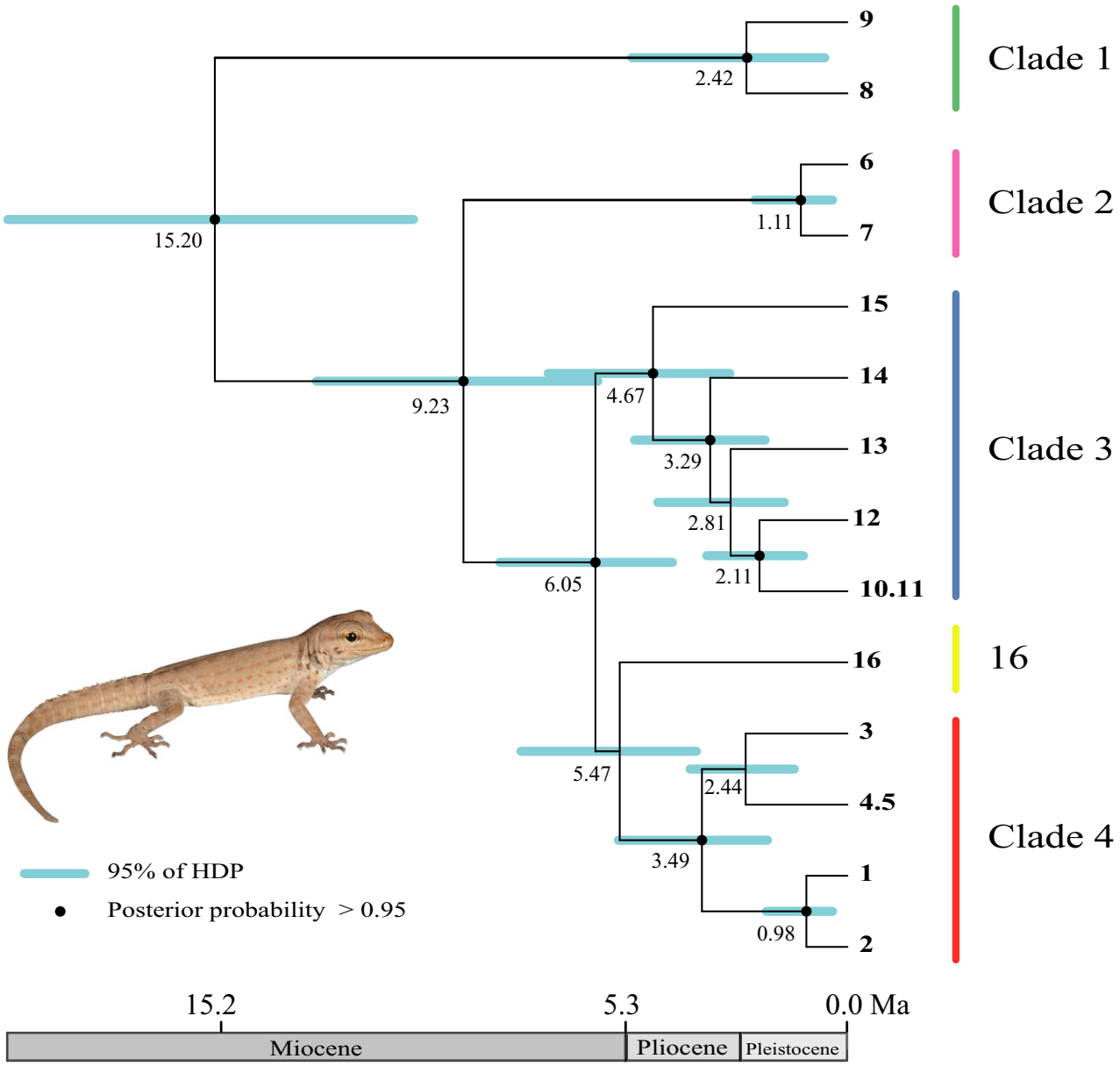

Figure 2 Time-calibrated multilocus coalescent-based species tree of *Pristurus rupestris rupestris* inferred in *BEAST with data set 2 (two mitochondrial and four nuclear genes, 2459 bp) and supported by the BP&P species delimitation analysis. Numbers at nodes indicate the mean divergence time and bars represent the 95% high posterior density interval of the time estimates. Filled circles at nodes indicate posterior probability support values > 0.95. The photograph is *P. r. rupestris* from candidate species 7. See Supporting information for more information on the genes, parameters and calibrations used.

robust and slender phenotypes are differentiated, most candidate species within each of these morphotypes are indistinguishable.

DISCUSSION

This study uncovers an unparalleled degree of species-level diversification in an Arabian vertebrate, identifying 14 candidate species within a single subspecies of gecko inhabiting an area of less than 25,000 km^2. This illustrates the unknown diversity yet to be discovered in the planet's desert regions. Moreover, these results highlight the role of mountain ranges in generating and preserving diversity in arid environments (Sanders *et al.*, 2003; McCain, 2007). Mountains provide numerous possibilities for smaller scale geographical isolation of demes and allopatric speciation, particularly during periods of orogeny (Antonelli *et al.*, 2009), a relationship that has been detected in a number of groups (Liu *et al.*, 2006; Antonelli *et al.*, 2009; Bunce *et al.*, 2009; Toussaint *et al.*, 2014; Merckx *et al.*, 2015), and has probably contributed significantly to cladogenesis in *P. r. rupestris*. Indeed, most of its diversification occurred during the latter stages of

© 2017 John Wiley & Sons Ltd

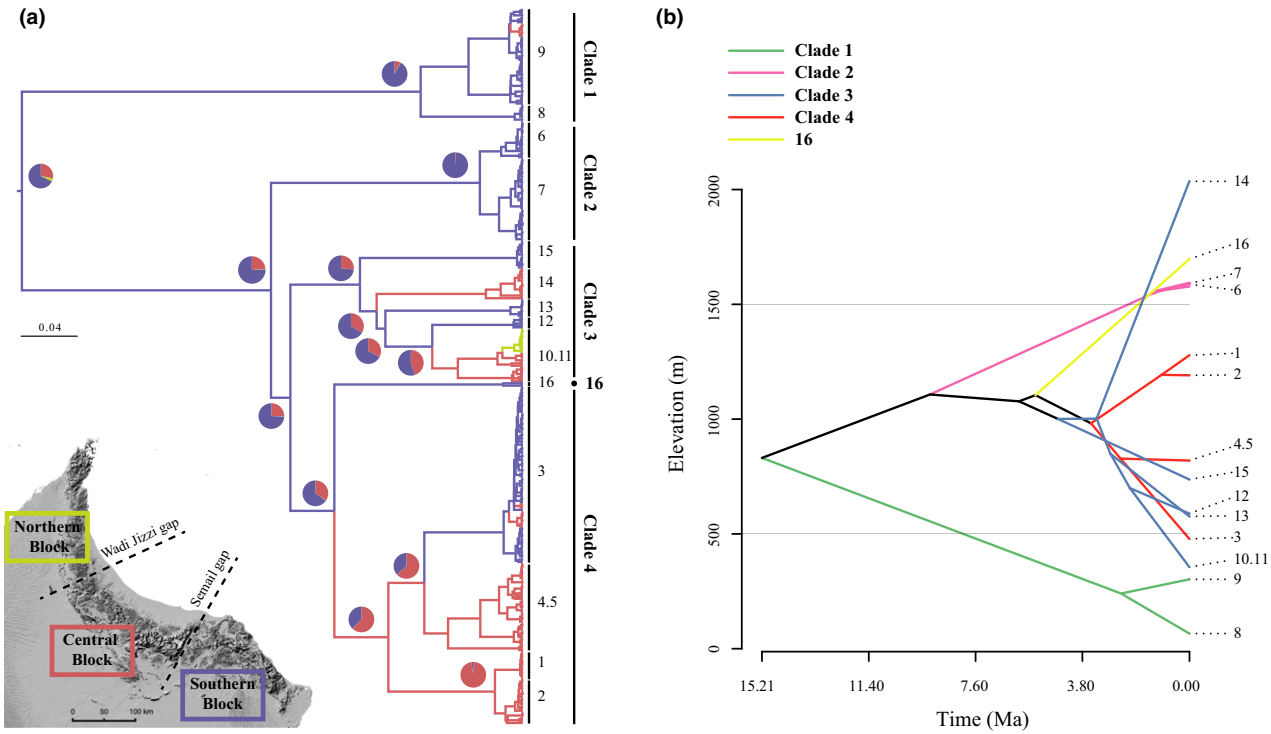

Figure 3 Map of the Hajar Mountains of south-eastern Arabia showing the geographical and altitudinal distribution of the 14 candidate species of *Pristurus rupestris rupestris*. (a) BEAST summary tree of *P. r. rupestris* using the BSSVS method of ancestral area reconstruction. Branch colour indicates inferred ancestral range (southern block, central block or northern block). A pie chart describing the probability of each inferred area is presented near the relevant nodes. A more detailed version of this figure with the probability values is shown in Fig. S5. (b) Altitudinal diversification through time of *P. r. rupestris*, based on ancestral state reconstructions of the elevation in the nodes.

mountain uplift, beginning in the late Miocene and continuing through the Pliocene and Quaternary, a time when elevations increased from 200 to 500 m (Kusky *et al.*, 2005). The appearance of new climatic environments and topographic discontinuities, combined with repeated altitudinal shifts of biotic communities during arid (glacial) and pluvial (interglacial) phases of the Arabian Pleistocene (Burns *et al.*, 2001) likely stimulated multiple dispersal events from areas of origin and fragmented populations into isolated demes leading to genetic divergence. Consistent with this, most of the sister candidate species date from the early and middle Pleistocene (Fig. 2).

Our ancestral area reconstruction (Fig. 3a and see Fig. S5) suggests that range expansion first initiated in the southern block and later proceeded northward, a pattern also reported for *Trachydactylus hajarensis* (de Pous *et al.*, 2016), and *Asaccus gallagheri* (work in progress), two gecko species endemic to the Hajar Mountains. During their movements towards north, Clades 3 and 4 have independently crossed the Semail gap to the central block, creating an assemblage of polyphyletic candidate species on both mountain blocks.

Several lineages have undergone genetic divergence and morphological diversification along elevational gradients (Figs 3 & 4). High altitudes were reached three times independently, and a robust morphology has convergently evolved consisting of wide heads, wide scapular and pelvic girdles, short legs and short axilla-groin lengths. Nevertheless, the morphospace of the majority of the candidate species greatly overlaps within the robust and slender phenotypes, resulting in a high degree of crypsis.

The lowlands (< 500 m), which are occupied by candidate species 8 and 9 (clade 1), have been independently colonized two times by high-altitude ancestors, candidate species 3 (clade 3) and 10.11 (clade 4). This pattern illustrates that mountains are not only centres of diversification (Toussaint *et al.*, 2014), but also act as 'species pumps', as taxa disperse into the surrounding lowlands (Wollenberg *et al.*, 2008).

Similar radiations of genetically divergent but morphologically cryptic populations may evolve in other lizards living on widespread but similarly coloured substrates that cover geologically unstable and irregular mountain topographies. In fact, radiations of cryptic mountain taxa have been reported for the lacertid lizards of the genus *Atlantolacerta* (Barata *et al.*, 2012a, 2014) the diurnal geckos of the genus *Quedenfeldtia* (Barata *et al.*, 2012b) and the nocturnal geckos of the genus *Ptyodactylus* (Perera & Harris, 2010) from the Atlas Mountains, and more recently for the extensive radiation of the *Ptyodactylus* species complex across the main mountain ranges of Arabia (Metallinou *et al.*, 2015).

© 2017 John Wiley & Sons Ltd

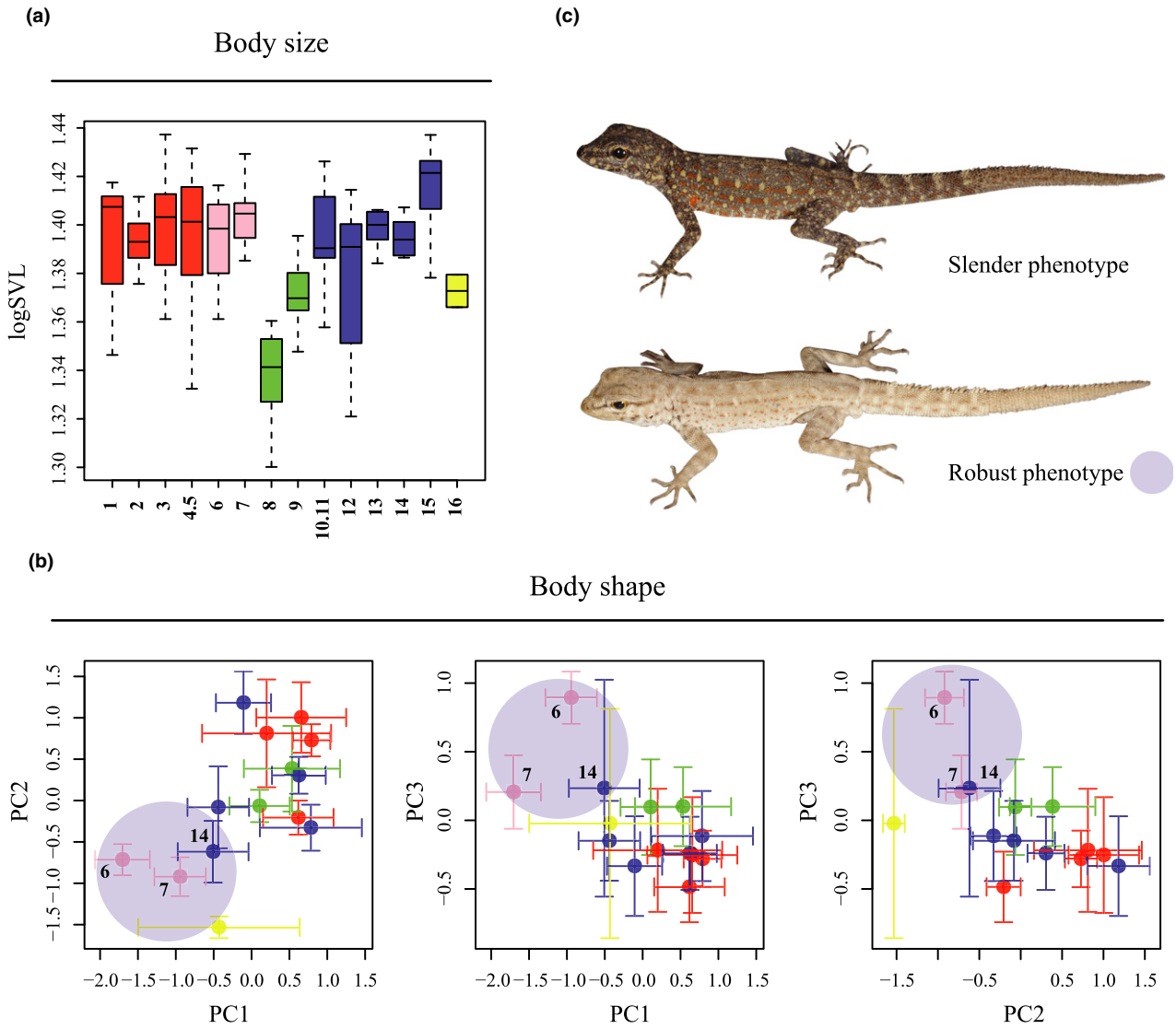

Figure 4 (a) Boxplot showing the $\log_{10}$SVL variation of the 14 candidate species of *Pristurus rupestris rupestris* and (b) their morphospace. The morphospace was obtained from the three first components of a PCA (reflecting 58% of the total variation) performed on 10 body measurements. The three robust phenotypes of *P. r. rupestris* are indicated by their candidate species codes. (c) The slender (candidate species 12) and robust (candidate species 7) phenotypes.

Overall, our results stress the importance of mountain ranges as centres of speciation and diversification, especially when compared to the surrounding low elevation arid environments, where reduced ecological complexity and extreme climatic conditions limit biodiversity. Thus, previous and ongoing research indicate that the Hajar Mountains are a biological hotspot and an important reservoir of diversity, and therefore should be a priority conservation focal point (Arnold & Gallagher, 1977 and other articles in the same volume; Carranza & Arnold, 2012; Carranza *et al.*, 2016; de Pous *et al.*, 2016). For example, candidate species 9, 3, 4.5 and 10.11 have wide distributions, but the remaining 10 candidate species appear to have very restricted ranges, sometimes being known from a single valley or slope and are likely populations of high conservation concern (see Fig. S4). The cryptic diversity discovered in *P. r. ruprestris* not only points to the need for a taxonomic revision, but it also highlights the problems faced by conservation planners. Without knowledge of the hidden biodiversity in a region like the Hajar Mountains, it is not possible to make meaningful conservation plans to protect these evolutionarily significant units. Similar analytical methodology, and importantly, fine-scale sampling is likely to uncover unknown diversity even in the most widespread and common species.

ACKNOWLEDGEMENTS

We wish to thank Fèlix Amat, David Donaire, Elena Gómez-Díaz, Roberto Sindaco, Jiri Smid, Pilar Dueñas and Aimar Ferran for assisting in sample collection and to Josep

© 2017 John Wiley & Sons Ltd

Roca for his great laboratory help. Special thanks are due to Saleh Al Saadi, Mohammed Al Shariani, Thuraya Al Sariri, Ali Al Kiyumi, Mohammed Abdullah Al Maharmi and the other members of the Nature Conservation Department of the Ministry of Environment and Climate Affairs, Sultanate of Oman and to the Centre for Environmental Studies and Research from the Sultan Qaboos University for their help and support and for issuing all the necessary permits. Sampling of *Pristurus* geckos was done with permission of the Nature Conservation Department of the Ministry of Environment and Climate Affairs, Sultanate of Oman (permit numbers 08/2005; 16/2008; 38/2010; 12/2011; 12/2013; 13/2013; 21/2013; 37/2014). This work was funded by grants CGL2012-36970 and CGL2015-70390-P from the Ministerio de Economía y Competitividad, Spain (co-funded by FEDER) and with support from the project 'Field study for the conservation of reptiles in Oman' Ministry of Environment and Climate Affairs (Ref: 22412027). J.G.P., M.S.R. and S.C. are members of the Grup de Recerca Consolidat of the Generalitat de Catalunya: 2014SGR1532. J.G.P. was supported by a JAE predoctoral grant from the CSIC, Spain and M.S.R. is funded by a FPI grant from the Ministerio de Economía y Competitividad, Spain (BES-2013-064248).

REFERENCES

Antonelli, A., Nylander, J.A.A., Persson, C. & Sanmartín, I. (2009) Tracing the impact of the Andean uplift on Neotropical plant evolution. *Proceedings of the National Academy of Sciences USA*, **106**, 9749–9754.

Arnold, E.N. (1980) The scientific results of the Oman flora and fauna survey 1977 (Dhofar). The reptiles and amphibians of Dhofar, southern Arabia. *Journal of Oman Studies, Special Report*, **2**, 273–332.

Arnold, E.N. (1986) A key and annotated checklist to the lizards and amphisbaenians of Arabia. *Fauna of Saudi Arabia*, **8**, 385–435.

Arnold, E.N. (1993) Historical changes in the ecology and behaviour of semaphore geckos (*Pristurus*, Gekkonidae) and their relatives. *Journal of Zoology*, **229**, 353–384.

Arnold, E.N. (2009) Relationships, evolution and biogeography of Semaphore geckos, *Pristurus* (Squamata, Sphaerodactylidae) based on morphology. *Zootaxa*, **2060**, 1–21.

Arnold, E.N. & Gallagher, M.D. (1977) Reptiles and amphibians from the mountains of northern Oman with special reference to the Jebel Akhdar region. The scientific results of the Oman flora and fauna survey 1975. *Journal of Oman Studies, Special Report*, **1**, 59–80.

Badiane, A., Garcia-Porta, J., Červenka, J., Kratochvíl, L., Sindaco, R., Robinson, M.D., Morales, H., Mazuch, T., Price, T., Amat, F., Shobrak, M.Y., Wilms, T., Simó-Riudalbas, M., Ahmadzadeh, F., Papenfuss, T.J., Cluchier, A., Viglione, J. & Carranza, S. (2014) Phylogenetic relationships of Semaphore geckos (Squamata: Sphaerodactylidae: *Pristurus*) with an assessment of the taxonomy of *Pristurus rupestris*. *Zootaxa*, **3835**, 33–58.

Barata, M., Carranza, S. & Harris, D.J. (2012a) Extreme genetic diversity in the lizard *Atlantolacerta andreanskyi* (Werner, 1929): a montane cryptic species complex. *BMC Evolutionary Biology*, **12**, 167.

Barata, M., Perera, A., Martínez-Freiría, F. & Harris, D.J. (2012b) Cryptic diversity within the Moroccan endemic day geckos *Quedenfeldtia* (Squamata: Gekkonidae): a multidisciplinary approach using genetic, morphological and ecological data. *Biological Journal of the Linnean Society*, **106**, 828–850.

Barata, M., Perera, A. & Harris, D.J. (2014) Cryptic variation in the Moroccan high altitude lizard *Atlantolacerta andreanskyi* (Squamata: Lacertidae). *African Journal of Herpetology*, **64**, 1–17.

Barraclough, T.G. & Vogler, A. (2000) Detecting the geographical pattern of speciation from species-level phylogenies. *The American Naturalist*, **155**, 419–434.

Brinkmann, K., Patzelt, A., Dickhoefer, U., Schlecht, E. & Buerkert, A. (2009) Vegetation patterns and diversity along an altitudinal and a grazing gradient in the Jabal al Akhdar mountain range of northern Oman. *Journal of Arid Environments*, **73**, 1035–1045.

Brito, J.C., Godinho, R., Martínez-Freiría, F. *et al.* (2014) Unravelling biodiversity, evolution and threats to conservation in the Sahara-Sahel. *Biological Reviews*, **89**, 215–231.

Bunce, M., Worthy, T.H., Phillips, M.J., Holdaway, R.N., Willerslev, E., Haile, J., Shapiro, B., Scofield, R.P., Drummond, A., Kamp, P.J.J. & Cooper, A. (2009) The evolutionary history of the extinct ratite moa and New Zealand Neogene paleogeography. *Proceedings of the National Academy of Sciences USA*, **106**, 20646–20651.

Burns, S.J., Fleitmann, D., Matter, A., Neff, U. & Mangini, A. (2001) Speleothem evidence from Oman for continental pluvial events during interglacial periods. *Geology*, **29**, 623–626.

Busais, S.M. & Joger, U. (2011) Three new species and one new subspecies of *Hemidactylus* Oken, 1817 from Yemen (Squamata, Gekkonidae). *Vertebrate Zoology*, **61**, 267–280.

Cadena, C.D., Kozak, K.H., Gómez, J.P., Parra, J.L., McCain, C.M., Bowie, R.C.K., Carnaval, A.C., Moritz, C., Rahbek, C., Roberts, T.E., Sanders, N.J., Schneider, C.J., VanDerWal, J., Zamudio, K.R. & Graham, C.H. (2012) Latitude, elevational climatic zonation and speciation in New World vertebrates. *Proceedings of the Royal Society B: Biological Sciences*, **279**, 194–201.

Carranza, S. & Arnold, E.N. (2012) A review of the gecko genus *Hemidactylus* (Squamata: Gekkonidae) from Oman based on morphology, mitochodrial and nuclear data, with descriptions of eight new species. *Zootaxa*, **95**, 1–95.

Carranza, S., Simó-Riudalbas, M., Jayasinghe, S., Wilms, T. & Els, J. (2016) Microendemicity in the northern Hajar Mountains of Oman and the United Arab Emirates with the description of two new species of geckos of the genus *Asaccus* (Squamata: Phyllodactylidae). *PeerJ*, **4**, e2371.

© 2017 John Wiley & Sons Ltd

de Pous, P., Machado, L., Metallinou, M., Červenka, J., Kratochvíl, L., Paschou, N., Mazuch, T., Šmíd, J., Simó-Riudalbas, M., Sanuy, D. & Carranza, S. (2016) Taxonomy and biogeography of *Bunopus spatalurus* (Reptilia; Gekkonidae) from the Arabian Peninsula. *Journal of Zoological Systematics and Evolutionary Research*, **54**, 67–81.

Dray, S. & Dufour, A.-B. (2007) The ade4 package: implementing the duality diagram for ecologists. *Journal of Statistical Software*, **22**, 1–20.

Drummond, A. & Rambaut, A. (2007) BEAST: Bayesian evolutionary analysis by sampling trees. *BMC Evolutionary Biology*, **7**, 214.

Ezard, T., Fujisawa, T. & Barraclough, T.G. (2009) *SPLITS: species' limits by threshold statistics*. R package version, 1.0-11/r29. http://R-Forge.R-project.org/projects/splits/

Fuchs, J., Fjeldså, J. & Bowie, R.C.K. (2011) Diversification across an altitudinal gradient in the Tiny Greenbul (*Phyllastrephus debilis*) from the Eastern Arc Mountains of Africa. *BMC Evolutionary Biology*, **11**, 117.

Fujisawa, T. & Barraclough, T.G. (2013) Delimiting species using single-locus data and the Generalized Mixed Yule Coalescent approach: a revised method and evaluation on simulated data sets. *Systematic Biology*, **62**, 707–724.

Gamble, T., Bauer, A.M., Greenbaum, E. & Jackman, T.R. (2008) Evidence for Gondwanan vicariance in an ancient clade of gecko lizards. *Journal of Biogeography*, **35**, 88–104.

Gamble, T., Bauer, A.M., Colli, G.R., Greenbaum, E., Jackman, T.R., Vitt, L.J. & Simons, A.M. (2011) Coming to America: multiple origins of New World geckos. *Journal of Evolutionary Biology*, **24**, 231–244.

Gamble, T., Greenbaum, E., Jackman, T.R., Russell, A.P. & Bauer, A.M. (2012) Repeated origin and loss of adhesive toepads in geckos. *PLoS ONE*, **7**, e39429.

Garcia-Porta, J., Morales, H.E., Gómez-Díaz, E., Sindaco, R. & Carranza, S. (2016) Patterns of diversification in islands: A comparative study across three gecko genera in the Socotra Archipelago. *Molecular Phylogenetics and Evolution*, **98**, 288–299.

Ghazanfar, S.A. (1991) Vegetation structure and phytogeography of Jabal Shams, an arid mountain in Oman. *Journal of Biogeography*, **18**, 299–309.

Heled, J. & Drummond, A.J. (2010) Bayesian inference of species trees from multilocus data. *Molecular Biology and Evolution*, **27**, 570–580.

Hugall, A.F., Foster, R. & Lee, M.S.Y. (2007) Calibration choice, rate smoothing, and the pattern of tetrapod diversification according to the long nuclear gene RAG-1. *Systematic Biology*, **56**, 543–563.

IUCN (2016) *The IUCN Red List of Threatened Species*. Version 2016-3. http://www.iucnredlist.org.

Jones, M.E.H., Anderson, C.L., Hipsley, C.A., Müller, J., Evans, S.E. & Schoch, R.R. (2013) Integration of molecules and new fossils supports a Triassic origin for Lepidosauria (lizards, snakes, and tuatara). *BMC Evolutionary Biology*, **13**, 208.

Katoh, K. & Toh, H. (2008) Recent developments in the MAFFT multiple sequence alignment program. *Briefings in Bioinformatics*, **9**, 286–298.

Kohler, T. & Maselli, D. (eds) (2012) *Mountains and climate change – from understanding to action*, 3rd edn. Published by Geographica Bernensia with the support of the Swiss Agency for Development and Cooperation (SDC), and an international team of contributors, Bern.

Kozak, K.H. & Wiens, J.J. (2007) Climatic zonation drives latitudinal variation in speciation mechanisms. *Proceedings of the Royal Society B: Biological Sciences*, **274**, 2995–3003.

Kumar, S., Stecher, G. & Tamura, K. (2016) MEGA7: Molecular Evolutionary Genetics Analysis version 7.0 for bigger datasets. *Molecular Biology and Evolution*, **33**, 1870–1874.

Kusky, T., Robinson, C. & El-Baz, F. (2005) Tertiary-Quaternary faulting and uplift in the northern Oman Hajar Mountains. *Journal of the Geological Society*, **162**, 871–888.

Lemey, P., Rambaut, A., Drummond, A. & Suchard, M. (2009) Bayesian phylogeography finds its roots. *PLoS Computational Biology*, **5**, e1000520. doi:10.1371/journal.pcbi.1000520.

Liu, J.-Q., Wang, Y.-J., Wang, A.-L., Hideaki, O. & Abbott, R.J. (2006) Radiation and diversification within the *Ligularia-Cremanthodium-Parasenecio* complex (Asteraceae) triggered by uplift of the Qinghai-Tibetan Plateau. *Molecular Phylogenetics and Evolution*, **38**, 31–49.

Mandaville, J. (1977) The scientific results of the Oman flora and fauna survey 1975. Plants. *Journal Oman Studies Special Report*, **1**, 229–267.

McCain, C.M. (2007) Could temperature and water availability drive elevational species richness patterns? A global case study for bats. *Global Ecology and Biogeography*, **16**, 1–13.

Merckx, V.S.F.T., Hendriks, K.P., Beentjes, K.K., *et al.* (2015) Evolution of endemism on a young tropical mountain. *Nature*, **524**, 347–350.

Metallinou, M., Červenka, J., Crochet, P.-A., Kratochvíl, L., Wilms, T., Geniez, P., Shobrak, M.Y., Brito, J.C. & Carranza, S. (2015) Species on the rocks: systematics and biogeography of the rock-dwelling *Ptyodactylus* geckos (Squamata: Phyllodactylidae) in North Africa and Arabia. *Molecular Phylogenetics and Evolution*, **85**, 208–220.

Oksanen, J., Blanchet, F.G., Kindt, R., Legendre, P., Minchin, P.R., O'Hara, R.B., Simpson, G.L., Solymos, P., Stevens, M.H.H. & Wagner, H. (2013) *Package 'vegan." R Package*. https://github.com/vegandevs/vegan.

Olave, M., Solà, E. & Knowles, L.L. (2014) Upstream analyses create problems with DNA-based species delimitation. *Systematic Biology*, **63**, 263–271.

Pepper, M., Fujita, M.K., Moritz, C. & Keogh, J.S. (2011) Palaeoclimate change drove diversification among isolated mountain refugia in the Australian arid zone. *Molecular Ecology*, **20**, 1529–1545.

Perera, A. & Harris, D.J. (2010) Genetic variability within the Oudri's fan-footed gecko *Ptyodactylus oudrii* in North Africa assessed using mitochondrial and nuclear DNA

© 2017 John Wiley & Sons Ltd

sequences. *Molecular Phylogenetics and Evolution*, **54**, 634–639.

Pons, J., Barraclough, T.G., Gomez-Zurita, J., Cardoso, A., Duran, D.P., Hazell, S., Kamoun, S., Sumlin, W.D. & Vogler, A.P. (2006) Sequence-based species delimitation for the DNA taxonomy of undescribed insects. *Systematic Biology*, **55**, 595–609.

Pyron, R.A., Burbrink, F.T. & Wiens, J.J. (2013) A phylogeny and revised classification of Squamata, including 4161 species of lizards and snakes. *BMC Evolutionary Biology*, **13**, 93.

R Development Core Team (2014) *R: A Language and Environment for Statistical Computing*. Vienna, Austria : the R Foundation for Statistical Computing. ISBN: 3-900051-07-0. http://www.R-project.org/.

Randi, E., Lucchini, V., Armijo-Prewitt, T., Kimball, R.T., Braun, E.L. & Ligon, J.D. (2000) Mitochondrial DNA phylogeny and speciation in the tragopans. *The Auk*, **117**, 1003–1015.

Reid, N.M. & Carstens, B.C. (2012) Phylogenetic estimation error can decrease the accuracy of species delimitation: a Bayesian implementation of the general mixed Yule-coalescent model. *BMC Evolutionary Biology*, **12**, 196.

Revell, L.J. (2012) phytools: an R package for phylogenetic comparative biology (and other things). *Methods in Ecology and Evolution*, **3**, 217–223.

Rivas, L.R. (1964) A reinterpretation or the concepts "sympatric" and "allopatric" with proposal of the additional terms "syntopic" and "allotopic". *Systematic Zoology*, **13**, 42–43.

Sanders, N.J., Moss, J. & Wagner, D. (2003) Patterns of ant species richness along elevational gradients in an arid ecosystem. *Global Ecology and Biogeography*, **12**, 93–102.

Schweizer, M., Seehausen, O. & Hertwig, S.T. (2011) Macroevolutionary patterns in the diversification of parrots: effects of climate change, geological events and key innovations. *Journal of Biogeography*, **38**, 2176–2194.

Šmíd, J., Moravec, J., Kratochvíl, L., Nasher, A.K., Mazuch, T., Gvoždík, V. & Carranza, S. (2015) Multilocus phylogeny and taxonomic revision of the *Hemidactylus robustus* species group (Reptilia, Gekkonidae) with descriptions of three new species from Yemen and Ethiopia. *Systematics and Biodiversity*, **13**, 346–368.

Toussaint, E.F.A., Hall, R., Monaghan, M.T., Sagata, K., Ibalim, S., Shaverdo, H.V., Vogler, A.P., Pons, J. & Balke, M. (2014) The towering orogeny of New Guinea as a trigger for arthropod megadiversity. *Nature Communications*, **5**: 4001.

Uetz, P., Goll, J. & Hallerman, J. (2016) *The reptile database*. Available at: http://www.reptile–database.org (accessed October 2016).

Venables, W. & Ripley, B. (2002) *Modern applied statistics using S-PLUS*. Springer, New York, USA.

Vidal, N. & Hedges, S.B. (2005) The phylogeny of squamate reptiles (lizards, snakes, and amphisbaenians) inferred from nine nuclear protein-coding genes. *Comptes Rendus Biologies*, **328**, 1000–1008.

Vuilleumier, F. & Monasterio, M. (1986) *High altitude tropical biogeography*. Oxford University Press, Oxford.

Wiens, J.J., Kozak, K.H. & Silva, N. (2013) Diversity and niche evolution along aridity gradients in North American lizards (Phrynosomatidae). *Evolution*, **67**, 1715–1728.

Wollenberg, K.C., Vieites, D.R., Van Der Meijden, A., Glaw, F., Cannatella, D.C. & Vences, M. (2008) Patterns of endemism and species richness in Malagasy cophyline frogs support a key role of mountainous areas for speciation. *Evolution*, **62**, 1890–1907.

Yang, Z. & Rannala, B. (2010) Bayesian species delimitation using multilocus sequence data. *Proceedings of the National Academy of Sciences USA*, **107**, 9264–9269.

Yousofi, S., Rastegar-Pouyani, E. & Hojati, V. (2015) Phylogenetic relationships among populations of *Pristurus rupestris* Blanford, 1874 (Sauria: Sphaerodactylidae) in southern Iran. *Turkish Journal of Zoology*, **39**, 1–6.

SUPPORTING INFORMATION

Additional Supporting Information may be found in the online version of this article:

Appendix S1 Extended methods.
Appendix S2 Supplementary tables.
Appendix S3 Supplementary figures.

DATA ACCESSIBILITY

All sequences generated for this study are deposited in GenBank with accession numbers listed in the supporting information (see Tables S1 and S2). All specimen measurements are available in Table S3.

BIOSKETCH

One of the main research lines of the Systematics, Biogeography and Evolution of Reptiles and Amphibians lab at the Institute of Evolutionary Biology (CSIC-Pompeu Fabra University) in Barcelona, Spain is the study of the processes that shape biodiversity across space and time, using Afro-Arabian reptiles as model organisms.

http://molevol.cmima.csic.es/carranza/index.html

Author contributions: J.G.P. and S.C. conceived the study; J.G.P., M.R. and S.C. collected samples; M.S.R. carried out the molecular lab work; J.G.P. and M.S.R. measured specimens and carried out the phylogenetic analyses; J.G.P. carried out the statistical analyses, all authors drafted the manuscript and gave final approval for publication.

Editor: Peter Linder

© 2017 John Wiley & Sons Ltd

Journal of Biogeography

SUPPORTING INFORMATION

Diversification in arid mountains: biogeography and cryptic diversity of the semaphore gecko *Pristurus rupestris rupestris* in Arabia

Joan Garcia-Porta, Marc Simó-Riudalbas, Michael Robinson and Salvador Carranza

Appendix S1: Extended methods. This section provides additional details on the laboratory protocols as well as statistical analysis, complementing information in the main Methods section.

DNA extraction and sequencing

Genomic DNA was extracted from ethanol-preserved tissue samples using the Qiagen DNeasy Blood & Tissue Kit (Qiagen, Valencia, CA, USA) or the SpeedTools Tissue DNA Extraction kit (Biotools, Madrid, Spain). A fragment of the 12S rRNA (*12S*) mitochondrial gene was PCR-amplified and sequenced in both directions for 466 samples using primers 12Sa and 12Sb – (Kocher *et al.,* 1989) and the two new specific primers 12SaRUP (5'-CAA ACT AGG ATT AGA TAC CCT ACT ATG CYT AGA-3') and 12SbRUP (5'-GAG GGT GAC GGG CGG TGT GTA CKC GTC CC-3'). The GMYC method (see next section) was used as a preliminary approach to delimit deep mitochondrial lineages and to select a subset of 75 samples for further gene sampling. The selected specimens were sequenced for the mitochondrial gene encoding the cytochrome *b* (*cytb*) (*cytb*; primers Cytb1 and Cytb2 – (Kocher *et al.,* 1989)), and four nuclear fragments of the genes encoding the oocyte maturation factor Mos (*c-mos*; primers FUF and FUR – (Gamble *et al.,* 2008)), a short fragment of the recombination-activating gene 1 (*rag1*; primers F700 and R700 – (Bauer *et al.,* 2007)), the recombination-activating gene 2 (*rag2*; primers PyF1 and PyR – (Gamble *et al.,* 2008)) and the melano-cortin 1 receptor (*mc1r*) gene. PCR conditions used for the amplification of *12S* were: initial step of 94ºC, 5'; followed by 35 cycles of 94ºC, 45"; 52ºC 45"; 72ºC 80"; a final step of 72ºC, 5, and for all the other gene fragments are in (Šmíd *et al.,* 2013). Contig assembly and translation to aminoacids were done in Geneious 6.1.8 (Kearse *et al.,* 2012), and heterozygote sites were coded according to IUPAC ambiguity codes.

Data sets, partitions and models of sequence evolution

Multiple sequence alignment of the *12S* gene was performed with the online application of MAFFT 7 (http://www.ebi.ac.uk/Tools/msa/mafft) (Katoh & Toh, 2008) with default parameters. The protein coding genes (*cytb*, *c-mos, rag1, rag2*, and *mc1r*) were aligned using the translation alignment algorithm in the software Geneious 6.1.8. A total of four data sets were used in the analyses: 1) data set 1 was used for identification and delimitation of deep mitochondrial lineages and included 221 unique haplotypes resulting from the 466 *12S* sequences amplified for all the sampled specimens (see Table S1 below). The aligned data set 1 included 392 base pairs (bp); 2) data set 2 was used for multilocus coalescent-based species tree inference and species delimitation analyses with BP&P (see below) and included a total of 75 specimens sequenced for 2,459 bp (389 bp of *12S*, 306 bp of *cytb*, 411 bp of *c-mos*, 270 bp of *rag1*, 405 bp of *rag2*, 669 bp of *mc1r*) (see Table S1 below); 3) data set 3 was used for dating the radiation of *P. r. rupestris* and consisted of 449 terminals including one representative of each one of the 14 candidate species of *P. r. rupestris* plus 435 different species downloaded from GenBank, with representatives of 117 out of the 123 accepted gecko genera (Uetz *et al.,* 2016). To download the GenBank sequences we BLASTed (Altschul *et al.,* 1997) all six genes from data set 2 against all gecko sequences available in GenBank. We then retrieved the longest sequence for each species of gecko with the additional requirement that sequences had to contain 200 bp or more (the search in GenBank was conducted during March 2014). We then opted for excluding the nuclear

gene *mc1r* due to its low number of hits in GenBank. For the remaining five genes, in order to minimize the amount of missing data, we included the sequences of all gecko species from GenBank for which at least three out of the five genes were available. Poorly aligned regions in the *12S* alignment were eliminated with Gblocks (Castresana, 2000) under low stringency options (Talavera & Castresana, 2007). The final alignment included a total of 449 terminals and 1,614 bp (234 bp of *12S*, 306 bp of *cytb*, 375 bp of *c-mos*, 291 bp of *rag1*, 408 bp of *rag2*) (see Table S2 below); 4) Data set 4 was used to infer the phylogeographic history and reconstruct the ancestral origin of *P. r. rupestris* in the Hajar Mountains with the Bayesian Stochastic Search Variable Selection (BSSVS; Lemey et al. 2009) of the discrete phylogeographic model as implemented in BEAST 1.8.0 (see below) and included all 466 specimens sequenced for the *12S* gene (392 bp);

Models of sequence evolution for the four data sets were inferred with jModelTest v2.1.3 (Guindon & Gascuel, 2003; Darriba *et al.,* 2012) under the AIC information criterion. For the *12S* alignment of data sets 1 and 4 the model selected was GTR+I+G; for data set 2 the models selected were GTR+G for the *12S* and *cytb*, HKY+I for the *c-mos*, *rag1* and *rag2*; and HKY+I+G for the *mc1r*; for data set 3 models selected were GTR+I+G for *12S*, *cytb*, *rag1* and *rag2* and TN93+I+G for *c-mos*. For the multilocus data sets 2 and 3 partitions were by gene in order to obtain the evolutionary rate of each one of the five genes after the analysis (data set 3) and to use it as a prior for the calibrated species tree (data set 2).

Phylogenetic analyses

Data sets 1 and 4 included *12S* sequences only (221 and 466 sequences, respectively) and were analysed with Bayesian Inference (BI) in BEAST 1.8.0 (Drummond & Rambaut, 2007). Three individual runs of $5x10^7$ generations were carried out, sampling at intervals of 10,000 generations. Models and prior specifications applied were as follows (otherwise by default): model of sequence evolution for the *12S* GTR+I+G; constant size coalescent tree prior; uncorrelated log-normal clock prior; random starting tree; base substitution prior Uniform (0,100); alpha prior Uniform (0,10). Posterior trace plots and effective sample sizes (ESS) of the runs were monitored in Tracer v1.5 (Rambaut & Drummond, 2013) to ensure convergence. The results of the individual runs were combined in LogCombiner discarding 10% of the samples and the maximum clade credibility (MCC) ultrametric tree was produced with TreeAnnotator (both provided with the BEAST package). BI analyses of data set 3 were performed in BEAST with the same parameters and tree priors as above but incorporating the appropriate models of sequence evolution for each one of the five genes (see above) and a Yule process tree prior. Species trees using data set 2 were inferred with *BEAST (Heled & Drummond, 2010) as implemented in the package BEAST 1.8.0. This method essentially implements a multispecies coalescent model to estimate the species tree from multiple genes and multiple individuals per species, while taking into account incomplete lineage sorting (Ruane *et al.,* 2013). For this analysis, nuclear data were phased using the program PHASE 2.1 (Stephens *et al.,* 2001; Stephens & Scheet, 2005) and input/output files were interconverted with SeqPHASE (Flot *et al.,* 2010) with

phase probabilities set at 0.7. Two individual runs of $10x10^7$ generations were carried out, sampling at intervals of 5,000 generations.

Species delimitation analysis

The species delimitation followed two steps. In a first step deep mitochondrial lineages within *P. r. rupestris* were objectively identified and delimited with data set 1 (*12S* sequences, haplotypes only) using the general mixed Yule-coalescent model (GMYC) (Pons *et al.,* 2006; Fujisawa & Barraclough, 2013). This model essentially detects the most likely tree depth (in the single-threshold approach) at which the pattern of tree branching shifts between a Yule process (reflecting inter-specific phylogenetic structure) and a coalescent process (reflecting intra-specific structure). The analysis was performed using the package "splits" (Ezard *et al.,* 2009) in R (R Development Core Team, 2014). Because inference of lineages relies on point estimates of the topology and branch lengths, the associated phylogenetic error could decrease the accuracy of delimitation results. Therefore, we assessed uncertainty in phylogenetic tree estimation and model parameters with a Bayesian implementation of the GMYC model, which integrates over these potential sources of error via MCMC simulation (Reid & Carstens, 2012). We used the R package “bGMYC” to calculate marginal posterior probabilities of lineage limits from the posterior distribution of ultrametric trees reconstructed with BEAST. A post-burn-in sample of 250 trees resampled from that posterior was used to calculate the posterior distribution of the GMYC model. We ran the bGMYC analysis for 100,000 generations with a burn-in of 10,000 generations.

The multilocus coalescent-based species delimitation with data set 2 was run with the program Bayesian Phylogenetics and Phylogeography (BP&P) 2.2 (Yang & Rannala, 2010). This program essentially uses a reversible-jump Markov chain Monte Carlo (rjMCMC) to estimate whether two or more lineages in a given species tree can be differentiated from each other accounting for the coalescent uncertainty provided by multiple independent loci. This method is very robust when multiple specimens and independent loci are used, even when migration rates exist between species (Zhang *et al.,* 2011). However, this approach is very sensitive to the phylogenetic tree used to guide the species delimitation algorithm (Leache & Fujita, 2010). For this reason, in our analyses we used the species tree of the GMYC/bGMYC mitochondrial lineages inferred in *BEAST as a guide tree. The BP&P analysis was based solely on the nuclear loci, which allowed us to evaluate the mitochondrial delimitation hypothesis (GMYC/bGMYC) with loci not used to generate it. We ran six different types of analyses, each one having a different combination of prior settings and rjMCMC algorithms. We used the two types of algorithms available in the program BP&P (0 and 1). The prior settings used followed previous studies (Leache & Fujita, 2010; Burbrink *et al.,* 2011; Cox *et al.,* 2012; Ruane *et al.,* 2013). The prior distributions of ancestral population sizes and root age were parameterized using a gamma distribution with the following combinations of alpha and beta parameters: large ancestral populations sizes and deep divergences (alpha = 1, beta = 10 for both priors); small ancestral populations and shallow divergences (alpha = 2, beta = 2000 for both priors) and finally, large ancestral population sizes (alpha = 1, beta = 10) with shallow divergences (alpha = 2,

beta= 2000). Each combination of prior settings and algorithms was run in two independent rjMCMC chains, for 500,000 generations, each time using a random species delimitation scheme as starting point. All runs were monitored during the initial few thousand generations to assess whether the acceptance proportions for the MCMC moves were in the recommended range between 0.3 and 0.7. If in some of the runs any acceptance proportion was outside this range, the runs were stopped and the finetune variables were modified accordingly before restarting the runs. After confirming convergence and good mixing in each of the analysis, we evaluated the posterior probabilities (pp) of all putative speciation events recovered in our guide tree. Any putative speciation event presenting a pp < 0.95 in at least one of the runs was considered as not reliable and its descendant tips were collapsed into the same species.

Calibration analyses

Data set 3 was used to infer a time-tree of Gekkota. The phylogenetic analysis was conducted by means of the package BEAST v1.8.0 following the same settings and parameters as above but including five calibration points that were used to estimate branch lengths in units of time:

1. The onset of the diversification in the Caribbean genus *Sphaerodactylus*. This calibration was set to a minimum of 20 Ma based on an amber fossil from the Dominican Republic (Daza & Bauer, 2012). The maximum age of this radiation was set conservatively to a soft maximum of 70 Ma, using a gamma distribution (α=2, β=10).
2. The split between *Teratoscincus scincus* and the clade formed by *T. przewalskii* and *T. roborowskii* was set to an age of 10 Ma (with a standard deviation of 1 Ma), assuming a vicariance event resulting from the uplift of the Tien Shan-Pamir Mountains in western China (Macey *et al.,* 1999).
3. The initiation of the diplodactyloid radiation in New Caledonia was placed as a soft maximum of 37 Ma, because geological and biological data show that the island was probably under water until this time (Nattier *et al.,* 2011; Pillon, 2012; Garcia-Porta & Ord, 2013; Papadopoulou *et al.,* 2013). A normal distribution with a mean at 20 Ma and a standard deviation of 10 Ma was used to set the prior of this calibration point.
4. The split between *Phelsuma ornata* from Mauritius and *Phelsuma inexpectata* from Reunion islands. This event was set to a soft maximum of 8.9 Ma based on the age of the oldest rocks of Mauritius, the oldest island in the Mascarenes (Moore *et al.,* 2011). The prior was set by an exponential distribution with an offset of 0 and a mean at 3 Ma.
5. Finally, the deepest split in the diplodactyloid radiation of New Zealand was set to a minimum of 19 Ma, based on the oldest fossils of geckos in the archipelago (Lee *et al.,* 2009) with a conservative soft maximum of 65 Ma. The prior was set by a gamma distribution (α=3, β=7).

In order to obtain the species tree inferred with data set 2 in units of time, we implemented in our *BEAST analysis the substitution rates for *12S*, *cytb*, *c-mos*, *rag1*

and *rag2* genes and the age of the root of the *P. r. rupestris* radiation obtained from the BEAST analysis of data set 3 above.

Genetic variability analysis

Uncorrected genetic distances (*p*-distances) of the *12S* mitochondrial gene for the 14 candidate species were inferred using MEGA 5 (Tamura *et al.,* 2011) with pairwise deletion using data set 1.

References

Altschul, S.F., Madden, T.L., Schäffer, A.A., Zhang, J., Zhang, Z., Miller, W. & Lipman, D.J. (1997) Gapped BLAST and PSI-BLAST: a new generation of protein database search programs. *Nucleic acids research*, **25**, 3389–3402.

Bauer, A.M., de Silva, A., Greenbaum, E. & Jackman T. (2007) A new species of day gecko from high elevation in Sri Lanka, with a preliminary phylogeny of Sri Lankan Cnemaspis (Reptilia, Squamata, Gekkonidae). *Zoosystematics and Evolution*, **83**, 22–32.

Burbrink, F.T., Yao, H., Ingrasci, M., Bryson, R.W., Guiher, T.J. & Ruane, S. (2011) Speciation at the Mogollon Rim in the Arizona mountain kingsnake (*Lampropeltis pyromelana*). *Molecular Phylogenetics and Evolution*, **60**, 445–454.

Castresana, J. (2000) Selection of Conserved Blocks from Multiple Alignments for Their Use in Phylogenetic Analysis. *Molecular Biology and Evolution*, **17**, 540–552.

Cox, C.L., Rabosky, A.R.D., Reyes-Velasco, J., Ponce-Campos, P., Smith, E.N., Flores-Villela, O. & Campbell, J.A. (2012) Molecular systematics of the genus *Sonora* (Squamata: Colubridae) in central and western Mexico. *Systematics and Biodiversity*, **10**, 93–108.

Darriba, D., Taboada, G.L., Doallo, R. & Posada, D. (2012) jModelTest 2: more models, new heuristics and parallel computing. *Nature methods*, **9**, 772.

Daza, J.D. & Bauer, A.M. (2012) A new amber-embedded sphaerodactyl gecko from Hispaniola, with comments on morphological synapomorphies of the Sphaerodactylidae. *Breviora*, **529**, 1–28.

Drummond, A. & Rambaut, A. (2007) BEAST: Bayesian evolutionary analysis by sampling trees. *BMC Evolutionary Biology*, **7**, 214.

Ezard, T., Fujisawa, T. & Barraclough, T.G. (2009) SPLITS: species' limits by threshold statistics. *R package version*, .

Flot, J.-F., Couloux, A. & Tillier, S. (2010) Haplowebs as a graphical tool for delimiting species: a revival of Doyle's "field for recombination" approach and its application to the coral genus *Pocillopora* in Clipperton. *BMC Evolutionary Biology*, **10**, 372.

Fujisawa, T. & Barraclough, T.G. (2013) Delimiting species using single-locus data and the Generalized Mixed Yule Coalescent approach: a revised method and evaluation on simulated data sets. *Systematic biology*, **62**, 707–24.

Gamble, T., Bauer, A.M., Greenbaum, E. & Jackman, T.R. (2008) Evidence for Gondwanan vicariance in an ancient clade of gecko lizards. *Journal of Biogeography*, **35**, 88–104.

Garcia-Porta, J. & Ord, T.J. (2013) Key innovations and island colonization as engines of evolutionary diversification: a comparative test with the Australasian diplodactyloid geckos. *Journal of evolutionary biology*, **26**, 2662–2680.

Guindon, S. & Gascuel, O. (2003) A simple, fast, and accurate algorithm to estimate large phylogenies by maximum likelihood. *Systematic biology*, **52**, 696–704.

Heled, J. & Drummond, A.J. (2010) Bayesian Inference of Species Trees from Multilocus Data. *Molecular Biology and Evolution*, **27**, 570–580.

Katoh, K. & Toh, H. (2008) Recent developments in the MAFFT multiple sequence alignment program. *Briefings in Bioinformatics*, **9**, 286–298.

Kearse, M., Moir, R., Wilson, A., Stones-Havas, S., Cheung, M., Sturrock, S., Buxton, S., Cooper, A., Markowitz, S., Duran, C., Thierer, T., Ashton, B., Meintjes, P. & Drummond, A. (2012) Geneious Basic: an integrated and extendable desktop software platform for the organization and analysis of sequence data. *Bioinformatics*, **28**, 1647–9.

Kocher, T.D., Thomas, W.K., Meyer, A., Edwards, S.V, Pääbo, S., Villablanca, F.X. & Wilson, A.C. (1989) Dynamics of mitochondrial DNA evolution in animals: amplification and sequencing with conserved primers. *Proceedings of the National Academy of Sciences*, **86**, 6196–6200.

Leache, A.D. & Fujita, M.K. (2010) Bayesian species delimitation in West African forest geckos (*Hemidactylus fasciatus*). *Proceedings of the Royal Society Biological Sciences*, **277**, 3071–3077.

Lee, M.S.Y., Hutchinson, M.N., Worthy, T.H., Archer, M., Tennyson, A.J.D., Worthy, J.P. & Scofield, R.P. (2009) Miocene skinks and geckos reveal long-term conservatism of New Zealand's lizard fauna. *Biology letters*, rsbl20090440.

Lemey, P., Rambaut, A., Drummond, A. & Suchard, M. (2009) Bayesian phylogeography finds its roots. PLoS Computational Biology 5, e1000520. doi:10.1371/journal.pcbi.1000520.

Macey, J.R., Wang, Y., Ananjeva, N.B., Larson, A. & Papenfuss, T.J. (1999) Vicariant patterns of fragmentation among gekkonid lizards of the genus Teratoscincus produced by the Indian collision: a molecular phylogenetic perspective and an area cladogram for Central Asia. *Molecular Phylogenetics and Evolution*, **12**, 320–332.

Moore, J., White, W.M., Paul, D., Duncan, R.A., Abouchami, W. & Galer, S.J.G.

(2011) Evolution of shield-building and rejuvenescent volcanism of Mauritius. *Journal of Volcanology and Geothermal Research*, **207**, 47–66.

Nattier, R., Robillard, T., Desutter-Grandcolas, L., Couloux, A. & Grandcolas P. (2011) Older than New Caledonia emergence? A molecular phylogenetic study of the eneopterine crickets (Orthoptera: Grylloidea). *Journal of Biogeography*, **38**, 2195–2209.

Papadopoulou, A., Cardoso, A. & Gómez-Zurita, J. (2013) Diversity and diversification of Eumolpinae (Coleoptera: Chrysomelidae) in New Caledonia. *Zoological Journal of the Linnean Society*, **168**, 473–495.

Pillon, Y. (2012) Time and tempo of diversification in the flora of New Caledonia. *Botanical Journal of the Linnean Society*, **170**, 288–298.

Pons, J., Barraclough, T.G., Gomez-Zurita, J., Cardoso, A., Duran, D.P., Hazell, S., Kamoun, S., Sumlin, W.D. & Vogler A.P. (2006) Sequence-based species delimitation for the DNA taxonomy of undescribed insects. *Systematic Biology*, **55**, 595–609.

Rambaut, A. & Drummond, A.J. (2013) Tracer v1. 5 Available from http://beast. bio. ed. ac. uk/Tracer. .

Reid, N.M. & Carstens, B.C. (2012) Phylogenetic estimation error can decrease the accuracy of species delimitation: a Bayesian implementation of the general mixed Yule-coalescent model. *BMC Evolutionary Biology*, **12**, 196.

Ruane, S., Bryson, R.W., Pyron, R.A. & Burbrink, F.T. (2013) Coalescent Species Delimitation in Milksnakes (Genus *Lampropeltis*) and Impacts on Phylogenetic Comparative Analyses. *Systematic Biology*, **63**, 231–250.

Šmíd, J., Carranza, S., Kratochvíl, L., Gvoždík, V., Nasher, A.K. & Moravec, J. (2013) Out of Arabia: A Complex Biogeographic History of Multiple Vicariance and Dispersal Events in the Gecko Genus *Hemidactylus* (Reptilia: Gekkonidae). *PLoS ONE*, **8**, e64018.

Stephens, M. & Scheet, P. (2005) Accounting for Decay of Linkage Disequilibrium in Haplotype Inference and Missing-Data Imputation. *The American Journal of Human Genetics*, **76**, 449–462.

Stephens, M., Smith, N.J. & Donnelly, P. (2001) A New Statistical Method for Haplotype Reconstruction from Population Data. *The American Journal of Human Genetics*, **68**, 978–989.

Talavera, G. & Castresana, J. (2007) Improvement of Phylogenies after Removing Divergent and Ambiguously Aligned Blocks from Protein Sequence Alignments. *Systematic Biology*, **56**, 564–577.

Tamura, K., Peterson, D., Peterson, N., Stecher, G., Nei M. & Kumar, S. (2011) MEGA5: Molecular Evolutionary Genetics Analysis Using Maximum Likelihood,

Evolutionary Distance, and Maximum Parsimony Methods. *Molecular Biology and Evolution*, **28**, 2731–2739.

Uetz, P., Goll, J. & Hallerman, J. (2015) The reptile database. <http://www.reptile–database.org> (accessed October 2016).

Yang, Z. & Rannala, B. (2010) Bayesian species delimitation using multilocus sequence data. *Proceedings of the National Academy of Sciences*, **107**, 9264–9269.

Zhang, C., Zhang, D.-X., Zhu, T. & Yang, Z. (2011) Evaluation of a Bayesian Coalescent Method of Species Delimitation. *Systematic Biology*, **60**, 747–761.

Journal of Biogeography

SUPPORTING INFORMATION

Diversification in arid mountains: biogeography and cryptic diversity of the semaphore gecko *Pristurus rupestris rupestris* in Arabia

Joan Garcia-Porta, Marc Simó-Riudalbas, Michael Robinson and Salvador Carranza

Appendix S2: Supplementary tables (Tables S1–S7)

Table S1. Information on the *Pristurus rupestris rupestris* specimens included in the phylogenetic (specimen code) and morphological (morphology = yes) analyses, with precise locality data (lat. and long.) and GenBank accession numbers. Candidate species refer to the 14 candidate species recognized by the BP&P analysis of dataset 2.

Can. species	Spec. code	Country	Lat.	Long.	Morpho.	*12S*	*cytb*	*c-mos*	*mc1r*	*rag1*	*rag2*
1	CN190	Oman	23,0753	57,6056	yes	KY023454					
1	CN4018	Oman	22,9257	57,6666	yes	KY023455					
1	CN4246	Oman	22,9257	57,6666	yes	KY023456					
1	S6035	Oman	23,0799	57,6130		KY023457	KY023856	KY023908	KY023995	KY024045	KY024118
1	S6064	Oman	22,9743	57,7000	yes	KY023458	KY023858	KY023890	KY023996	KY024046	KY024119
1	S6067	Oman	22,9963	57,7039		KY023459					
1	S6076	Oman	23,0092	57,6985		KY023460					
1	S6101	Oman	23,0799	57,6130		KY023461	KY023857	KY023891	KY024009	KY024047	KY024120
1	S6120	Oman	22,9819	57,7006		KY023462					
1	S6121	Oman	22,9711	57,6963		KY023463					
1	S6134	Oman	22,9232	57,6798	yes	KY023464	KY023859	KY023892		KY024048	
1	S7291	Oman	22,9743	57,7000		KY023465					
1	S7352	Oman	22,9743	57,7000		KY023466					
1	S7652b	Oman	22,9326	57,6691		KY023467					
1	S7792	Oman	22,9743	57,7000		KY023468					
1	S7802	Oman	22,9743	57,7000		KY023469					
1	S7809	Oman	23,0912	57,7335	yes	KY023470					
2	AO6	Oman	23,0564	57,4669		KY023471					
2	AO65	Oman	23,1403	57,4103		KY023472					
2	AO7	Oman	23,0564	57,4669		KY023473					
2	AO8	Oman	23,0564	57,4669		KY023474					
2	CN4055	Oman	23,0311	57,3245		KY023475					
2	CN4237	Oman	23,0311	57,3245	yes	KY023476					
2	CN6975	Oman	23,0311	57,3245	yes	KY023477					
2	S7239	Oman	23,1003	57,1192	yes	KY023478	KY023860	KY023905	KY024008	KY024086	KY024155
2	S7245	Oman	23,1186	57,0958	yes	KY023479	KY023861	KY023906	KY023998	KY024087	KY024156
2	S7270	Oman	23,1244	57,4566		KY023480					
2	S7273	Oman	23,1323	57,4617	yes	KY023481					
2	S7285	Oman	23,1186	57,0958		KY023482					
2	S7297	Oman	23,1323	57,4617		KY023483					
2	S7303	Oman	23,1186	57,0958		KY023484					
2	S7368	Oman	23,1012	57,4424		KY023485					
2	S7408	Oman	23,1865	57,1389		KY023486					
2	S7438	Oman	23,1865	57,1389		KY023487	KY023862	KY023893	KY024013	KY024049	
2	S7463	Oman	23,1865	57,1389		KY023488					
2	S7468	Oman	23,1244	57,4566		KY023489					
2	S7477	Oman	23,0811	57,3504		KY023490					
2	S7489	Oman	23,1255	57,4043	yes	KY023491					
2	S7573	Oman	23,1255	57,4043		KY023492					
2	S7622	Oman	23,1040	57,3545		KY023493					
2	S7702	Oman	23,0349	57,3160	yes	KY023494		KY023909		KY024050	

2	S7743	Oman	23,0796	57,4224		KY023495
2	S7745	Oman	23,0796	57,4224		KY023496
2	S7777	Oman	23,1012	57,4424		KY023497
2	S7896	Oman	23,0811	57,3504		KY023498
2	S7901	Oman	23,1012	57,4424		KY023499
2	S9020	Oman	23,1040	57,3545		KY023500
3	AO5	Oman	23,6047	58,3603		KY023501
3	CN108	Oman	23,6996	57,7757		KY023502
3	CN169	Oman	23,1317	58,6189		KY023503
3	CN176	Oman	23,1317	58,6189		KY023504
3	CN179	Oman	22,8469	59,1381	yes	KY023505
3	CN212	Oman	23,1317	58,6189		KY023506
3	CN3590	Oman	22,8964	59,1601		KY023507
3	CN3705	Oman	22,9088	59,1715	yes	KY023508
3	CN3720	Oman	22,8947	59,1401	yes	KY023509
3	CN3997	Oman	22,9166	59,1910	yes	KY023510
3	CN4004	Oman	22,6896	59,3526		KY023511
3	CN4044	Oman	23,1317	58,6189		KY023512
3	CN4048	Oman	23,1317	58,6189		KY023513
3	CN4052	Oman	23,1317	58,6189		KY023514
3	CN4175	Oman	23,1317	58,6189	yes	KY023515
3	CN68	Oman	23,6643	57,9010		KY023516
3	CN6997	Oman	23,1317	58,6189		KY023517
3	CN7147	Oman	23,1317	58,6189	yes	KY023518
3	CN7171	Oman	23,1317	58,6189		KY023519
3	CN7208	Oman	23,1317	58,6189		KY023520
3	CN7282	Oman	23,1317	58,6189		KY023521
3	CN80	Oman	23,6531	57,8794		KY023522
3	CN8046	Oman	23,1317	58,6189		KY023523
3	CN8218	Oman	22,9073	59,1768		KY023524
3	CN8653	Oman	23,1317	58,6189		KY023525
3	CN8956	Oman	23,1317	58,6189		KY023526
3	CN8972	Oman	23,1317	58,6189	yes	KY023527
3	CN8983	Oman	23,1317	58,6189		KY023528
3	CN98	Oman	23,1317	58,6189		KY023529
3	S1673	Oman	23,4603	58,5866	yes	KY023530
3	S1689	Oman	22,8106	59,2499	yes	KY023531
3	S1691	Oman	22,8106	59,2499		KY023532
3	S1754	Oman	22,8106	59,2499		KY023533
3	S1762	Oman	23,5117	58,6446		KY023534
3	S1773	Oman	23,5117	58,6446	yes	KY023535
3	S1797	Oman	22,8106	59,2499		KY023536
3	S1799	Oman	23,5117	58,6446	yes	KY023537
3	S5719	Oman	23,5894	58,1651		KY023538
3	S586	Oman	23,5117	58,6446		KY023539
3	S6038	Oman	23,5894	58,1651		KY023540

3	S6039	Oman	23,5894	58,1651		KY023541					
3	S6040	Oman	23,5894	58,1651		KY023542					
3	S6100	Oman	22,4966	59,3970	yes	KY023543		KY023894	KY024002	KY024051	KY024121
3	S6108	Oman	23,4094	58,1003		KY023544					
3	S6115	Oman	23,7453	57,7325		KY023545					
3	S6131	Oman	23,5894	58,1651		KY023546					
3	S6135	Oman	23,0858	59,0467		KY023547					
3	S6140	Oman	23,5894	58,1651		KY023548					
3	S7049	Oman	23,1060	58,6444		KY023549					
3	S7065	Oman	22,8699	59,1834		KY023550		KY023895	KY024005	KY024052	KY024122
3	S7068	Oman	23,5546	58,1875		KY023551					
3	S7070	Oman	23,0773	58,6477		KY023552					
3	S7082	Oman	23,1060	58,6444		KY023553					
3	S7083	Oman	23,1333	58,6520		KY023554					
3	S7177	Oman	23,1648	58,3853		KY023555					
3	S7197	Oman	23,1333	58,6520		KY023556					
3	S7214	Oman	22,6919	59,3561		KY023557					
3	S7218	Oman	22,7003	59,2954		KY023558					
3	S7232	Oman	22,7003	59,2954		KY023559					
3	S7247	Oman	22,8699	59,1834	yes	KY023560					
3	S7256	Oman	23,5894	58,1651		KY023561					
3	S7269	Oman	22,8733	59,1723		KY023562					
3	S7310	Oman	22,5390	59,3682		KY023563		KY023910	KY024003	KY024053	KY024123
3	S7351	Oman	22,7574	59,0940		KY023564					
3	S7398	Oman	23,2931	57,9775		KY023565					
3	S7409	Oman	23,7865	57,7961	yes	KY023566					
3	S7414	Oman	23,2931	57,9775		KY023567					
3	S7416	Oman	23,7865	57,7961		KY023568					
3	S7417	Oman	23,5870	58,1633		KY023569					
3	S7418	Oman	23,3103	57,9958		KY023570					
3	S7422	Oman	23,5137	57,8534		KY023571					
3	S7430	Oman	23,7547	57,5813		KY023572					
3	S7439	Oman	23,7865	57,7961		KY023573					
3	S7446	Oman	23,7865	57,7961		KY023574					
3	S7451	Oman	23,7881	57,7826		KY023575					
3	S7456	Oman	23,0858	59,0467		KY023576					
3	S7458	Oman	23,5493	57,4759		KY023577					
3	S7472	Oman	23,4685	58,1936		KY023578					
3	S7473b	Oman	22,8951	59,1376		KY023579					
3	S7481	Oman	23,0773	58,6477		KY023580					
3	S7493	Oman	23,0773	58,6477		KY023581					
3	S7525	Oman	23,1648	58,3853	yes	KY023582					
3	S7527	Oman	22,8237	59,0076		KY023583					
3	S7534	Oman	23,1317	58,6189	yes	KY023584	KY023872	KY023913	KY024007	KY024054	KY024124
3	S7535	Oman	23,1060	58,6444		KY023585					
3	S7543	Oman	22,8733	59,1723		KY023586	KY023876	KY023915	KY024006	KY024055	KY024125

3	S7544	Oman	22,8962	59,1443	yes	KY023587					
3	S7545	Oman	22,7914	59,2287		KY023588					
3	S7548	Oman	23,1060	58,6444		KY023589					
3	S7553	Oman	23,1317	58,6189	yes	KY023590	KY023873	KY023914	KY023999	KY024056	KY024126
3	S7561	Oman	22,8963	59,1602	yes	KY023591					
3	S7565	Oman	22,7625	58,8531		KY023592	KY023874	KY023917	KY024011	KY024057	KY024127
3	S7569	Oman	22,8848	59,1311		KY023593					
3	S7575	Oman	22,8848	59,1311		KY023594					
3	S7579	Oman	23,5546	58,1875		KY023595					
3	S7634	Oman	22,8962	59,1443		KY023596					
3	S7667	Oman	22,5122	59,3414		KY023597					
3	S7675	Oman	23,5894	58,1651		KY023598					
3	S7680	Oman	23,5903	58,4078		KY023599					
3	S7709	Oman	23,6159	58,5854	yes	KY023600					
3	S7729	Oman	23,0723	58,1867		KY023601					
3	S7738	Oman	23,4523	58,5053		KY023602					
3	S7749	Oman	23,7547	57,5813		KY023603					
3	S7787	Oman	23,3400	58,6254		KY023604					
3	S7803	Oman	23,4508	57,8653		KY023605					
3	S7818	Oman	23,3400	58,6254		KY023606					
3	S7864	Oman	23,6909	58,0394		KY023607					
3	S7874	Oman	23,3103	57,9958		KY023608					
3	S9000	Oman	23,1333	58,6520		KY023609					
3	S9016	Oman	22,8963	59,1602	yes	KY023610					
3	S9018	Oman	22,8333	58,9882	yes	KY023611	KY023875	KY023916	KY024034	KY024058	KY024128
3	UAE54	Oman	22,9164	58,8769		KY023612					
3	UAE55	Oman	22,9164	58,8769		KY023613					
3	UAE58	Oman	23,1081	58,5625	yes	KY023614					
3	UAE59	Oman	23,1081	58,5625		KY023615					
4.5	CN32	Oman	23,4014	57,4293	yes	KY023616					
4.5	CN3424	Oman	23,4014	57,4293	yes	KY023617					
4.5	CN3709	Oman	23,4014	57,4293	yes	KY023618					
4.5	CN375	Oman	23,3791	57,4498		KY023619					
4.5	CN5829	Oman	23,3902	57,2184	yes	KY023620					
4.5	S6046	Oman	23,2231	57,3752		KY023621					
4.5	S6116	Oman	23,7622	56,8941	yes	KY023622					
4.5	S6132	Oman	23,8720	56,9075	yes	KY023623		KY023896	KY024014	KY024059	KY024129
4.5	S7158	Oman	23,9522	56,7025	yes	KY023624	KY023863	KY023897	KY024016	KY024060	KY024130
4.5	S7181	Oman	23,2419	57,5418		KY023625					
4.5	S7182	Oman	23,1764	57,6523		KY023626		KY023898	KY024017	KY024061	KY024131
4.5	S7202	Oman	23,1764	57,6523		KY023627					
4.5	S7212	Oman	23,1829	57,4163		KY023628					
4.5	S7237	Oman	23,1771	57,4102		KY023629					
4.5	S7240	Oman	23,2180	57,3782		KY023630					
4.5	S7241	Oman	23,1829	57,4163		KY023631					
4.5	S7249	Oman	23,1990	57,3644	yes	KY023632	KY023865	KY023899	KY024000	KY024062	KY024132

4.5	S7251	Oman	23,1771	57,4102	yes	KY023633	KY023866	KY023900	KY024004	KY024063	KY024133
4.5	S7255	Oman	23,2444	57,3693	yes	KY023634	KY023867	KY023901	KY024015	KY024064	KY024134
4.5	S7266	Oman	23,1990	57,3644		KY023635					
4.5	S7296	Oman	23,1937	57,3948		KY023636					
4.5	S7400	Oman	23,4083	57,4238		KY023637					
4.5	S7403	Oman	23,3808	57,8229		KY023638					
4.5	S7406	Oman	23,3808	57,8229		KY023639					
4.5	S7412	Oman	23,3849	57,2389		KY023640					
4.5	S7421	Oman	23,2128	57,2041		KY023641					
4.5	S7425	Oman	23,4465	57,8804		KY023642					
4.5	S7432	Oman	23,3067	57,6958		KY023643					
4.5	S7433	Oman	23,8690	56,4023	yes	KY023644					
4.5	S7447	Oman	23,4355	57,3281		KY023645					
4.5	S7450	Oman	23,1961	57,1984		KY023646					
4.5	S7455	Oman	23,2377	57,1495		KY023647					
4.5	S7461	Oman	23,5334	57,3343	yes	KY023648					
4.5	S7462	Oman	23,4973	56,8993	yes	KY023649	KY023864	KY023907	KY024018	KY024088	
4.5	S7466	Oman	23,4083	57,4238		KY023650					
4.5	S7470	Oman	23,3901	57,8324		KY023651					
4.5	S7742	Oman	23,7705	56,3929		KY023652		KY023902	KY024019	KY024065	KY024135
4.5	S7768	Oman	23,3067	57,6958		KY023653					
4.5	S7822	Oman	23,4407	57,1189		KY023654					
4.5	S7828	Oman	23,4083	57,4238		KY023655					
4.5	S7831	Oman	23,2128	57,2041		KY023656					
4.5	S7838	Oman	23,5924	56,5549		KY023657					
4.5	S7841	Oman	23,3067	57,6958		KY023658					
4.5	S7842	Oman	23,4465	57,8804		KY023659					
4.5	S7856	Oman	23,4973	56,8993		KY023660					
4.5	S7861	Oman	23,3850	57,8363		KY023661					
4.5	S7873	Oman	23,3424	57,3133		KY023662					
4.5	S7880	Oman	23,4973	56,8993		KY023663					
4.5	S7889	Oman	23,3067	57,6958		KY023664					
4.5	S7892	Oman	23,4945	57,0354		KY023665					
4.5	S7894	Oman	23,7705	56,3929		KY023666					
4.5	S7900	Oman	23,3901	57,8324		KY023667					
4.5	S9021	Oman	23,3424	57,3133		KY023668					
4.5	S7159b	Oman	23,1477	57,7353	yes	KY023669	KY023868	KY023903	KY024010	KY024066	KY024136
4.5	S7161b	Oman	23,1477	57,7353		KY023670	KY023870	KY023911	KY023997	KY024067	KY024137
4.5	S7191	Oman	23,1473	57,7462		KY023671	KY023869	KY023904	KY024012	KY024068	KY024138
4.5	S7196	Oman	23,1782	57,7618	yes	KY023672	KY023871	KY023912	KY024001	KY024069	KY024139
4.5	S7209	Oman	23,1473	57,7462	yes	KY023673					
6	CN147	Oman	22,7171	59,2329		KY023674					
6	CN3580	Oman	22,7109	59,1571		KY023675					
6	CN3737	Oman	22,7056	59,2490	yes	KY023676					
6	CN6980	Oman	22,7056	59,2490	yes	KY023677					
6	CN7011	Oman	22,7056	59,2490		KY023678					

6	CN7096	Oman	22,7109	59,1571	yes	KY023679					
6	CN7112	Oman	22,7171	59,2329	yes	KY023680					
6	CN7168	Oman	22,7171	59,2329	yes	KY023681					
6	CN7181	Oman	22,7109	59,1571	yes	KY023682					
6	CN7198	Oman	22,7171	59,2329		KY023683					
6	CN7215	Oman	22,7171	59,2329	yes	KY023684					
6	CN7960	Oman	22,7109	59,1571	yes	KY023685					
6	CN8060	Oman	22,7171	59,2329		KY023686					
6	S7185	Oman	22,7033	59,2615	yes	KY023687	KY023847	KY023954	KY023983	KY024089	KY024157
6	S7186b	Oman	22,7111	59,1412		KY023688					
6	S7198	Oman	22,7033	59,2615	yes	KY023689					
6	S7201b	Oman	22,7172	59,2358	yes	KY023690					
6	S7203	Oman	22,7172	59,2358	yes	KY023691	KY023850	KY023958	KY023984	KY024090	KY024158
6	S7216	Oman	22,7033	59,2615	yes	KY023692					
6	S7231	Oman	22,7111	59,1412	yes	KY023693	KY023848	KY023956	KY023989	KY024091	KY024159
6	S7259	Oman	22,7176	59,2163	yes	KY023694					
6	S7507	Oman	22,7176	59,2163	yes	KY023695					
6	S7570	Oman	22,7176	59,2163	yes	KY023696					
6	S7813	Oman	22,7172	59,2358		KY023697	KY023849	KY023955	KY023990	KY024092	KY024160
7	CN127	Oman	22,8469	59,1381	yes	KY023698					
7	CN175	Oman	22,7102	59,1403	yes	KY023699					
7	CN3480	Oman	22,8656	59,1038	yes	KY023700					
7	CN3491	Oman	22,7102	59,1403	yes	KY023701					
7	CN3507	Oman	22,7102	59,1403	yes	KY023702					
7	CN3520	Oman	22,8656	59,1038		KY023703					
7	CN3587	Oman	22,8656	59,1038		KY023704					
7	CN3701	Oman	22,7395	59,1063		KY023705					
7	CN3992	Oman	22,7102	59,1403		KY023706					
7	CN4057	Oman	22,7102	59,1403		KY023707					
7	CN4161	Oman	22,7102	59,1403		KY023708					
7	CN4165	Oman	22,7102	59,1403	yes	KY023709					
7	CN4178	Oman	22,7102	59,1403		KY023710					
7	CN4188	Oman	22,7102	59,1403	yes	KY023711					
7	CN4241	Oman	22,7102	59,1403		KY023712					
7	CN7212	Oman	22,7102	59,1403	yes	KY023713					
7	CN7269	Oman	22,8656	59,1038	yes	KY023714					
7	CN8286	Oman	22,7102	59,1403	yes	KY023715					
7	CN8628	Oman	22,8656	59,1038		KY023716					
7	CN8960	Oman	22,7102	59,1403		KY023717					
7	S7188	Oman	22,7111	59,1412		KY023718					
7	S7193	Oman	22,8253	59,1117		KY023719					
7	S7200	Oman	22,8672	59,1763		KY023720	KY023851	KY023959	KY023986	KY024093	KY024161
7	S7211	Oman	22,7111	59,1412		KY023721					
7	S7219	Oman	22,8480	59,1387		KY023722					
7	S7225	Oman	22,8253	59,1117		KY023723					
7	S7226	Oman	22,7111	59,1412		KY023724					

7	S7228	Oman	22,8480	59,1387		KY023725					
7	S7229	Oman	22,7111	59,1412		KY023726					
7	S7264	Oman	22,8455	59,1383	yes	KY023727					
7	S7476	Oman	22,7058	59,1421		KY023728					
7	S7479	Oman	22,7180	59,1210		KY023729					
7	S7490	Oman	22,8825	59,1239		KY023730					
7	S7501	Oman	22,8825	59,1239		KY023731					
7	S7509	Oman	22,8255	59,0857		KY023732					
7	S7510	Oman	22,8255	59,0857	yes	KY023733					
7	S7511	Oman	22,7662	59,0337	yes	KY023734					
7	S7529	Oman	22,7180	59,1210	yes	KY023735					
7	S7531	Oman	22,8415	59,0977	yes	KY023736					
7	S7532	Oman	22,7058	59,1421		KY023737					
7	S7537	Oman	22,7396	59,1060		KY023738					
7	S7538	Oman	22,8204	59,0641		KY023739					
7	S7539	Oman	22,7058	59,1421	yes	KY023740	KY023852	KY023960	KY023985	KY024094	KY024162
7	S7542	Oman	22,8255	59,0857		KY023741					
7	S7547	Oman	22,7662	59,0337	yes	KY023742	KY023853	KY023961	KY023987	KY024095	KY024163
7	S7549	Oman	22,8204	59,0641		KY023743					
7	S7556	Oman	22,7396	59,1060	yes	KY023744					
7	S7560	Oman	22,7703	59,0758	yes	KY023745	KY023854	KY023957	KY023988	KY024096	KY024164
7	S7563	Oman	22,8415	59,0977		KY023746					
7	S7566	Oman	22,8825	59,1239		KY023747					
7	S7572	Oman	22,8255	59,0857		KY023748					
7	S7673b	Oman	22,7396	59,1060		KY023749					
7	S7756	Oman	22,7111	59,1412		KY023750					
7	S9017	Oman	22,8204	59,0641		KY023751					
8	CN159	Oman	22,8452	59,2412	yes	KY023752					
8	CN3588	Oman	22,8452	59,2412	yes	KY023753					
8	CN7971	Oman	22,8452	59,2412	yes	KY023754					
8	CN8037	Oman	22,8452	59,2412	yes	KY023755					
8	CN8965	Oman	22,8452	59,2412	yes	KY023756					
8	S7072	Oman	22,8448	59,2416		KY023757		KY023942	KY024021	KY024097	KY024165
8	S7187	Oman	22,9088	59,1715		KY023758	KY023877	KY023945	KY024022	KY024098	KY024166
8	S7508	Oman	22,8448	59,2416	yes	KY023759	KY023878	KY023946	KY024029	KY024099	KY024167
8	S7536	Oman	22,9088	59,1715		KY023760					
8	S7577	Oman	22,8448	59,2416	yes	KY023761					
8	S8000	Oman	22,8444	59,2419	yes	KY023762		KY023949	KY024031	KY024100	KY024168
9	AO20	Oman	22,7867	57,5939		KY023763					
9	CN145	Oman	22,2359	59,2262	yes	KY023764					
9	CN3597	Oman	22,7199	58,1495		KY023765					
9	CN4023	Oman	22,2359	59,2262	yes	KY023766					
9	CN7251	Oman	22,5709	59,0999		KY023767					
9	CN7266	Oman	22,2359	59,2262		KY023768					
9	S1540	Oman	22,3688	58,0591		KY023769					
9	S1645	Oman	23,0620	57,1304	yes	KY023770					

9	S1757	Oman	22,8108	57,6024		KY023771					
9	S1796	Oman	22,8108	57,6024		KY023772					
9	S1881	Oman	23,0620	57,1304		KY023773					
9	S1891	Oman	22,7896	57,5998	yes	KY023774					
9	S2126	Oman	22,7896	57,5998		KY023775					
9	S2137	Oman	22,7896	57,5998		KY023776					
9	S6111	Oman	22,6502	58,8628		KY023777					
9	S6113	Oman	22,7816	57,8513		KY023778					
9	S6114	Oman	22,2641	59,2583		KY023779					
9	S6117	Oman	22,5962	58,8243		KY023780					
9	S6125	Oman	23,0132	56,9797		KY023781					
9	S6146	Oman	22,5051	58,7481		KY023782					
9	S7165	Oman	22,2280	59,1852		KY023783					
9	S7171	Oman	22,7816	57,8513		KY023784					
9	S7204	Oman	22,6827	59,3256		KY023785					
9	S7246	Oman	22,4283	59,3562		KY023786	KY023879	KY023947	KY024027	KY024101	KY024169
9	S7276	Oman	22,3377	59,3113	yes	KY023787	KY023880	KY023939	KY024020	KY024070	KY024140
9	S7434	Oman	23,1183	56,7780		KY023788					
9	S7437	Oman	23,0961	57,3097	yes	KY023789					
9	S7457	Oman	23,0961	57,3097	yes	KY023790					
9	S7460	Oman	23,1397	57,8442		KY023791	KY023884	KY023952	KY024023	KY024102	KY024170
9	S7497	Oman	22,7510	59,3088		KY023792					
9	S7541	Oman	22,8333	58,9882	yes	KY023793	KY023887	KY023940	KY024032	KY024071	KY024141
9	S7552	Oman	22,7625	58,8531		KY023794	KY023888	KY023941	KY024026	KY024072	KY024142
9	S7564	Oman	22,4283	59,3562		KY023795					
9	S7590	Oman	22,4283	59,3562		KY023796					
9	S7669	Oman	22,5318	59,7622		KY023797					
9	S7706	Oman	22,4639	59,0520		KY023798					
9	S7708	Oman	21,8424	59,5667		KY023799					
9	S7716	Oman	22,3776	57,5140		KY023800					
9	S7717	Oman	21,9518	59,6082		KY023801					
9	S7719	Oman	21,8424	59,5667		KY023802	KY023881	KY023950	KY024024	KY024103	KY024171
9	S7721	Oman	21,8424	59,5667		KY023803					
9	S7727	Oman	22,8425	58,3909		KY023804					
9	S7737	Oman	21,9518	59,6082		KY023805					
9	S7744	Oman	23,1183	56,7780		KY023806					
9	S7753	Oman	21,9518	59,6082		KY023807					
9	S7763	Oman	21,8424	59,5667		KY023808					
9	S7778	Oman	22,5318	59,7622		KY023809					
9	S7797	Oman	22,5318	59,7622		KY023810					
9	S7849	Oman	22,6245	58,6566		KY023811					
9	S7853	Oman	23,0609	57,1307		KY023812					
9	S7865	Oman	23,3774	56,6817	yes	KY023813	KY023885	KY023948	KY024033	KY024104	KY024172
9	S7886	Oman	22,5318	59,7622		KY023814					
9	S7911	Oman	22,3776	57,5140		KY023815	KY023886	KY023951	KY024025	KY024105	KY024173
9	S7934	Oman	22,4386	58,7765		KY023816					

9	S7954	Oman	22,5880	58,6842		KY023817					
9	S8002	Oman	22,0396	59,3228		KY023818					
9	S9011	Oman	22,3377	59,3113		KY023819					
9	S9012	Oman	22,4283	59,3562	yes	KY023820	KY023882	KY023943	KY024030	KY024106	KY024174
9	S9013	Oman	22,5390	59,3682	yes	KY023821	KY023883	KY023944	KY024028	KY024107	KY024175
9	S9014	Oman	22,5227	59,4136		KY023822					
9	S9015	Oman	22,7510	59,3088		KY023823					
9	S9019	Oman	22,8738	58,9252		KY023824					
10.11	CN4244	Oman	23,5055	56,4916	yes	KY023359					
10.11	CN74	Oman	23,5413	56,3014		KY023360					
10.11	CN8298	Oman	23,5332	56,3177	yes	KY023361					
10.11	S7155b	Oman	24,0998	56,4756		KY023362					
10.11	S7166	Oman	24,3020	56,1275	yes	KY023363	KY023825	KY023889	KY023962	KY024035	
10.11	S7167b	Oman	24,6666	55,9649	yes	KY023364	KY023826	KY023918	KY023963	KY024036	KY024109
10.11	S7184b	Oman	24,2873	56,0982		KY023365					
10.11	S7207	Oman	24,2274	56,3249		KY023366					
10.11	S7215	Oman	24,5802	56,0502		KY023367					
10.11	S7220	Oman	24,4083	55,9968		KY023368					
10.11	S7233	Oman	24,3020	56,1275	yes	KY023369					
10.11	S7415	Oman	24,3614	56,7465	yes	KY023370	KY023828	KY023922	KY023968	KY024073	KY024143
10.11	S7420	Oman	23,5416	56,3017		KY023371					
10.11	S7424	Oman	23,5416	56,3017		KY023372	KY023827	KY023919	KY023967	KY024037	KY024110
10.11	S7426	Oman	23,5057	56,4643		KY023373					
10.11	S7443	Oman	24,3614	56,7465		KY023374					
10.11	S7659	UAE	24,8222	56,0698		KY023375					
10.11	SPM001302	UAE	25,2078	56,3275		KY023376					
10.11	SPM002883	Oman	24,6861	56,1575		KY023377					
10.11	SPM002894	UAE	25,2806	56,1864		KY023378					
10.11	UAE23	UAE	25,4167	56,1678		KY023379					
10.11	UAE24	UAE	25,4167	56,1678		KY023380					
10.11	UAE31	Oman	24,5153	56,4622	yes	KY023381					
10.11	UAE34	Oman	24,4514	56,2892	yes	KY023382					
10.11	UAE40	UAE	25,2256	56,3161	yes	KY023383					
10.11	CN111	Oman	23,4166	57,6690		KY023384					
10.11	CN116	Oman	23,3863	57,6605		KY023385					
10.11	CN133	Oman	23,4412	57,6609		KY023386	KY023829	KY023920	KY023964	KY024038	KY024111
10.11	CN56	Oman	23,3179	57,5923		KY023387					
10.11	CN58	Oman	23,4479	57,6611		KY023388					
10.11	CN69	Oman	23,3733	57,6658		KY023389					
10.11	CN99	Oman	23,4660	57,6721		KY023390					
10.11	S7401	Oman	23,3875	57,6593		KY023391			KY023969	KY024108	
10.11	S7407	Oman	23,3875	57,6593	yes	KY023392	KY023830		KY023966	KY024039	KY024112
10.11	S7882	Oman	23,3875	57,6593	yes	KY023393	KY023831	KY023926	KY023965	KY024040	KY024113
12	CN39	Oman	23,1749	57,8532	yes	KY023394					
12	CN4171	Oman	23,1749	57,8532	yes	KY023395					
12	S6060	Oman	23,1397	57,8442	yes	KY023396	KY023832	KY023932	KY023977	KY024074	KY024144

12	S7120	Oman	23,1701	57,8498	yes	KY023397	KY023833	KY023933	KY023978	KY024075	KY024145
12	S7452	Oman	23,1397	57,8442	yes	KY023398		KY023934	KY023980	KY024076	
12	S7475	Oman	23,1397	57,8442	yes	KY023399					
12	S7730	Oman	23,1750	57,8532	yes	KY023400	KY023834	KY023935	KY023974	KY024077	KY024146
13	CN3489	Oman	23,1432	58,4244	yes	KY023401					
13	CN3699	Oman	23,1432	58,4244	yes	KY023402					
13	CN4040	Oman	23,1432	58,4244		KY023403					
13	CN7213	Oman	23,1432	58,4244		KY023404					
13	CN7239	Oman	23,1432	58,4244	yes	KY023405					
13	CN7939	Oman	23,1432	58,4244		KY023406					
13	S6102	Oman	22,7177	58,1504	yes	KY023407	KY023839	KY023923	KY023971	KY024078	KY024147
13	S6123	Oman	22,9686	58,2930	yes	KY023408					
13	S7526	Oman	23,1431	58,4244	yes	KY023409	KY023840	KY023938	KY023970	KY024041	KY024114
13	S7533	Oman	23,1431	58,4244	yes	KY023410	KY023841	KY023928	KY023972	KY024042	KY024115
13	S7551	Oman	23,1431	58,4244	yes	KY023411	KY023842	KY023929	KY023981	KY024079	KY024148
13	S7599	Oman	23,1431	58,4244		KY023412					
14	AO30	Oman	23,0781	57,6064		KY023413					
14	AO48	Oman	23,1233	57,6156		KY023414					
14	AO55	Oman	23,0781	57,6064		KY023415					
14	CN4174	Oman	23,0794	57,6703	yes	KY023416					
14	CN7200	Oman	23,0794	57,6703	yes	KY023417					
14	S6036	Oman	23,0799	57,6130		KY023418	KY023835	KY023936	KY023975	KY024080	KY024149
14	S6079	Oman	23,0735	57,6675		KY023419					
14	S6083	Oman	23,0689	57,6414		KY023420					
14	S6087	Oman	23,0689	57,6414		KY023421					
14	S6088	Oman	23,0801	57,6143		KY023422	KY023836	KY023927	KY023973	KY024081	KY024150
14	S6089	Oman	23,0689	57,6414		KY023423					
14	S6093	Oman	23,0302	57,7022		KY023424					
14	S7284	Oman	22,9819	57,7006		KY023425					
14	S7288	Oman	23,1493	57,4625		KY023426					
14	S7294	Oman	23,1493	57,4625		KY023427					
14	S7312	Oman	23,1134	57,6597	yes	KY023428					
14	S7528	Oman	23,1493	57,4625	yes	KY023429	KY023838	KY023924	KY023982	KY024082	KY024151
14	S7718	Oman	23,0894	57,6820		KY023430					
14	S7736	Oman	23,0801	57,6143	yes	KY023431	KY023837	KY023925	KY023976	KY024083	KY024152
14	S7903	Oman	23,0894	57,6820		KY023432					
15	CN3717	Oman	22,6190	59,0935	yes	KY023433					
15	CN8031	Oman	22,6190	59,0935	yes	KY023434					
15	CN8289	Oman	22,6190	59,0935	yes	KY023435					
15	CN8662	Oman	22,6190	59,0935	yes	KY023436					
15	S6097	Oman	22,6016	59,0826		KY023437					
15	S6109	Oman	22,6016	59,0826		KY023438					
15	S6122	Oman	22,5088	59,1265	yes	KY023439	KY023843	KY023930	KY023993	KY024084	KY024153
15	S7175	Oman	22,6016	59,0826		KY023440					
15	S7258	Oman	22,7662	59,0337	yes	KY023441	KY023845	KY023937	KY023994	KY024085	KY024154
15	S7546	Oman	22,7703	59,0758	yes	KY023442	KY023846	KY023921	KY023991	KY024043	KY024116

15	S7714	Oman	22,6016	59,0826		KY023443					
15	S7739	Oman	22,6016	59,0826		KY023444					
15	S7833	Oman	22,5725	59,0945		KY023445					
15	S7967	Oman	22,6016	59,0826		KY023446					
15	S7989	Oman	22,6016	59,0826	yes	KY023447					
15	UAE44	Oman	22,6203	59,0931	yes	KY023448					
15	UAE45	Oman	22,6203	59,0931	yes	KY023449	KY023844	KY023931	KY023992		
15	UAE46	Oman	22,6203	59,0931		KY023450					
16	CN192	Oman	23,1317	58,6189		KY023451					
16	CN3704	Oman	23,1317	58,6189	yes	KY023452					
16	S7257	Oman	23,1317	58,6189	yes	KY023453	KY023855	KY023953	KY023979	KY024044	KY024117

Table S2. Species list and GenBank accession numbers for all the specimens of Gekkota included in the phylogenetic analysis of dataset 3.

Species	*12S*	*cytb*	*c-mos*	*rag1*	*rag2*
Aeluroscalabotes felinus	AB028746		HQ426517	HQ426259	HQ426432
Afroedura karroica			JQ945523	JQ945277	JQ945415
Afroedura loveridgei	DQ852695		AY172918	JQ945278	JQ945416
Afrogecko plumicaudus			JQ945525	JQ945279	JQ945417
Afrogecko porphyreus	DQ852696	EF490750	AY172919	EF490723	JQ945418
Afrogecko swartbergensis			JQ945527	JQ945280	JQ945419
Agamura persica	DQ852726	EU589176	KC191025	JX440675	JQ945420
Ailuronyx tachyscopaeus			JQ945529	JQ945282	JQ945421
Ailuronyx trachygaster			JQ945530	JQ945283	JQ945422
Alsophylax pipiens			JQ945531	JQ945284	JQ945423
Amalosia rhombifer			FJ855472	FJ855451	JQ945489
Aprasia parapulchella			AY134539	HQ426260	HQ426433
Aristelliger georgeensis	KC190934		KC191043	HQ426261	KC191141
Aristelliger lar			EF534931	EF534805	EF534973
Aristelliger praesignis			HQ426519	HQ426262	HQ426436
Asaccus platyrhynchus			EU293670	EU293625	EU293715
Bavayia cyclura			HQ426521	HQ426264	HQ426437
Bavayia geitaina			JQ945532	JX024469	JQ945424
Blaesodactylus antongilensis			JQ945534	EU054230	JQ945426
Bunopus tuberculatus	EU589158	EU589181	JQ945535	JX440676	JQ945427
Calodactylodes illingworthorum			JQ945536	JQ945288	JQ945428
Carphodactylus laevis	AF090175	AF109528	AF039467	FJ855442	EF534947
Chatogekko amazonicus		DQ104142	EU435231	HQ426268	JF416915
Chondrodactylus angulifer	DQ275403	AY123394	JQ945537	JQ945289	JQ945429
Chondrodactylus bibronii	DQ275406		EU293690	JN543930	EU293735
Chondrodactylus fitzsimonsi	DQ275404	AF449125		DQ275448	
Chondrodactylus turneri	DQ852708	AY221374	AY221332	DQ275449	
Christinus marmoratus	DQ852698		FJ855461	FJ855440	JQ945430
Cnemaspis africana			JQ945539	JQ945291	JQ945431
Cnemaspis dickersonae			JQ945540	JQ945292	JQ945432
Cnemaspis kandiana			JQ945541	JQ945293	JQ945433
Cnemaspis kendallii			AY172923	JQ945294	JQ945434
Cnemaspis limi	HQ896026	HQ896026	EF534935	EF534809	EF534977
Cnemaspis podihuna			JQ945543	JQ945295	JQ945435
Cnemaspis uzungwae			JQ945544	JQ945296	JQ945436
Coleodactylus brachystoma		DQ110710	EU435236	EF534792	EF534959
Coleodactylus septentrionalis		DQ110676	EU435258	EF534791	EF534958
Coleonyx brevis	AB308451		HQ426528	HQ426271	HQ426444
Coleonyx mitratus	AB028747		HQ426529	HQ426272	HQ426445
Coleonyx variegatus	AB114446	AB114446	EU116676	EF534777	EF534943
Colopus kochii	DQ275374	AY123398	JQ945545	JQ945297	JQ945437
Colopus wahlbergii	DQ275375	AY123395	JQ945546	JQ945298	JQ945438
Crenadactylus ocellatus			FJ571641	AY662627	JQ945439
Crossobamon orientalis	DQ852715	HM921200	JQ945547	JQ945299	JQ945440
Cryptactites peringueyi	DQ852718		JQ945548	JQ945300	JQ945441
Cyrtodactylus angularis			JQ945549	JQ945301	JQ945442
Cyrtodactylus ayeyarwadyensis		EU268380	JQ945550	EU268287	JQ945443
Cyrtodactylus fasciolatum	KC735096		KC735108	HM622351	
Cyrtodactylus irregularis			JQ945551	JQ945302	JQ945444
Cyrtodactylus jarujini			JQ945552	JQ945303	JQ945445
Cyrtodactylus novaeguineae			HQ426531	HQ426274	HQ426447
Cyrtodactylus philippinicus			JQ945553	JQ945304	JQ945446
Cyrtodactylus pulchellus	DQ852717		DQ852732	JX440711	
Cyrtopodion scabrum	KC735098	HM921199	KC735110	KC152025	HQ426448
Delma butleri			AY134548	HQ426276	HQ426449
Delma tincta	DQ852694		AY172926	HQ426277	HQ426450
Dierogekko insularis			JQ945555	JX024491	JQ945448

Diplodactylus conspicillatus			HQ426533	HQ426278	HQ426451
Diplodactylus tessellatus			FJ571639	FJ571624	JQ945449
Dixonius siamensis			JQ945557	EU054283	JQ945450
Dixonius vietnamensis			JQ945558	EU054281	JQ945451
Ebenavia inunguis	EU596608	EU596692	HQ256744	HQ426280	FJ830327
Elasmodactylus tetensis	DQ275407	AY026926	JQ945559	JQ945307	JQ945452
Elasmodactylus tuberculosus	DQ275408	AF449134		DQ275452	
Eublepharis macularius	AF090186		EU366458	EF534776	EF534942
Euleptes europaea	KC190935		KC191042	EF534806	KC191142
Eurydactylodes agricolae			JQ945560	GU459547	JQ945453
Geckoella triedrus	DQ852719		JQ945561	JX440682	JQ945454
Geckolepis maculata	EU596610	EU596693	JQ974167	EU054210	JQ945455
Geckolepis typica	JQ974129		JQ974159	EU054209	
Gehyra australis			JQ945563	JN019145	JQ945456
Gehyra dubia			JQ945565	JN393957	JQ945458
Gehyra mutilata	DQ852699	FJ830054	AY217853	JN393962	FJ830328
Gehyra nana			JQ945567	JN393965	JQ945460
Gehyra variegata	AF090185		FJ855460	FJ855439	JQ945461
Gekko badenii			JQ945569	JN019130	JQ945462
Gekko chinensis		EU417676	JQ945571	JN019123	JQ945464
Gekko gecko	HM370130	HM370130	EU366455	AY662625	EF534981
Gekko hokouensis	AF323511	EU417690		JN019125	
Gekko mindorensis			JQ945572	JN019140	JQ945465
Gekko monarchus			JQ945573	JN019141	JQ945466
Gekko subpalmatus		EU417696	JQ945574	JN019128	JQ945467
Gekko swinhonis	JQ906550	GQ131347		JN019126	
Gekko vittatus	AB178897		JQ945575	JN019136	JQ945468
Goggia lineata	AY763261		AY172930	JQ945310	JQ945469
Gonatodes albogularis	GU139931		GU139825	EF534797	EF534965
Gonatodes annularis	GU139914	JQ639547	GU139795	EF534794	EF534961
Gonatodes caudiscutatus			EF534920	EF534795	EF534962
Gonatodes ceciliae	GU139934		GU139828	JF416914	EF564114
Gonatodes concinnatus	GU139937		GU139831	HQ426282	EF564096
Gonatodes daudini	GU139938		GU139832	EF534793	EF534960
Gonatodes eladioi			EF564081	HQ426283	EF564107
Gonatodes hasemani	GU139940		GU139833		EF534963
Gonatodes humeralis	GU139941	JQ639585	EU435263	EF534796	EF534964
Gonatodes ocellatus	GU139945		GU139839	HQ426284	EF564098
Gonatodes vittatus	GU139946		GU139840	HQ426285	EF564112
Goniurosaurus araneus	AB308453		HQ426537	HQ426286	HQ426455
Goniurosaurus kuroiwae	AB028751	AB827798	HQ876393		
Goniurosaurus luii	EF081253		EF081254	HQ426287	HQ426456
Gymnodactylus amarali			JN935470	JN935429	JN935399
Haemodracon riebeckii			EU293672	EU293627	EU293717
Hemidactylus aaronbaueri	HM595676	HM595640		HM622352	
Hemidactylus albopunctatus	KC818657	KC818794	KC818745	KC818952	KC819017
Hemidactylus alkiyumii	JQ957094	KC818805	JQ957123	KC818955	JQ957401
Hemidactylus anamallensis	KC735101	HM595644	KC735113	KC735088	
Hemidactylus angulatus	EF202130	KC818813	KC818747	EU268306	KC819020
Hemidactylus barodanus	KC818668	KC818814	KC818750	KC818957	KC819021
Hemidactylus bouvieri	AF324808	DQ120250	AY863042		EF540731
Hemidactylus bowringii	AF323515	EU268405		HM622354	
Hemidactylus brasilianus	DQ120425	DQ120254	HQ426523	EU268290	HQ426439
Hemidactylus brookii	HM180306	HM921205	KC735118	GQ375314	
Hemidactylus citernii	KC818670	KC818815	JQ957124	KC818958	JQ957406
Hemidactylus dawudazraqi	KC818674	HQ833755	JQ957161	KC818959	JQ957442
Hemidactylus dracaenacolus	DQ120380	DQ120209	KC818752		KC819023
Hemidactylus fasciatus	DQ852724	EU268386	JQ945577	EU268309	JQ945470
Hemidactylus festivus	JQ957097	KC818821	JQ957125	KC818964	JQ957410
Hemidactylus flaviviridis	KF057086	KC818825	JQ957126	HM559694	KC819027
Hemidactylus forbesii	DQ120339	DQ120168	KC818756		

Hemidactylus foudaii	KC818677	DQ120214	KC818757	KC818968	JQ957413
Hemidactylus frenatus	GQ245970	GQ245970	EU116684	FJ855441	EF534982
Hemidactylus funaiolii	KC818678	KC818827	KC818758	KC818969	KC819030
Hemidactylus garnotii	DQ120459	EU268396		EU268302	
Hemidactylus giganteus	KF057088	HM559598	KC735120	HM622357	
Hemidactylus gracilis	HM595696	HM595659		HM622359	
Hemidactylus granchii	KC818679			KC818970	KC819031
Hemidactylus granosus	KF647571	KF647583	KF647576	KF647597	KF647607
Hemidactylus granti	DQ120381	DQ120210	KC818759		KC819033
Hemidactylus greeffii	DQ120415	EU268401	HQ426542	EU268308	HQ426459
Hemidactylus haitianus	DQ120387	HQ833764	HQ426543	HM559699	
Hemidactylus hajarensis	JQ957105	KC818829	JQ957128	KC818972	JQ957419
Hemidactylus homoeolepis	JQ957110	KC818832	JQ957131	KC818973	KC819034
Hemidactylus inexpectatus	JQ957066	JQ957205	JQ957140		JQ957426
Hemidactylus inintellectus	JQ982804	JQ982926	KC818766		KC819035
Hemidactylus isolepis	KC818680	KC818835	KC818769	KC818974	KC819036
Hemidactylus jumailiae	KC818682	KC818838	KC818770	KC818975	KC819037
Hemidactylus karenorum	DQ120464	DQ120293		EU268301	
Hemidactylus lavadeserticus	KC818684	HQ833746		KC818976	KC819039
Hemidactylus lemurinus	JQ957113	KC818839	JQ957137	KC818978	JQ957423
Hemidactylus leschenaultii	HM595698	HM921201		HM559701	
Hemidactylus longicephalus	DQ120416	HM559603	HQ426544	HM559703	HQ426460
Hemidactylus lopezjuradoi	EU730639	EU730651			EU730682
Hemidactylus luqueorum	JQ957107	JQ957213	JQ957145		JQ957430
Hemidactylus mabouia	HM180323	EU268393	KC818771	HQ426291	KC819040
Hemidactylus macropholis	DQ120343	DQ120172	JQ957138	HQ426292	JQ957424
Hemidactylus maculatus	HM595700	HM559607		HM622361	
Hemidactylus masirahensis	JQ957063	JQ957204	JQ957139		JQ957425
Hemidactylus mindiae	KC818686	HQ833748		KC818989	KC819041
Hemidactylus modestus	DQ120386	DQ120215	JQ957149		JQ957432
Hemidactylus ophiolepis	KC818689	KC818841	KC818772	KC818982	KC819042
Hemidactylus oxyrhinus	DQ120344	DQ120173	KC818774		KC819043
Hemidactylus palaichthus	DQ120434	EU268400	HQ426548	EU268307	HQ426464
Hemidactylus paucituberculatus	JQ957115	JQ957222	JQ957150		JQ957433
Hemidactylus persicus	KC818691	KC818843	KC818775	HM622362	KC819044
Hemidactylus platycephalus	KC818694	KC818845	KC818776	KC818985	KC819046
Hemidactylus platyurus	DQ120466	EU268384	HQ426530	HM622363	HQ426446
Hemidactylus prashadi	HM595704	HM559609		HM559709	
Hemidactylus pumilio	DQ120382	DQ120211	KC818777		KC819048
Hemidactylus robustus	KC818699	KC818854	KC818779	EU054271	JQ957436
Hemidactylus ruspolii	KC818706	KC818860	KC818782		KC819052
Hemidactylus saba	KF647567	KF647579	KF647573	KF647594	KF647605
Hemidactylus shihraensis	KC818708	KC818865	KC818783	KC818991	KC819053
Hemidactylus sinaitus	KC818714	KC818869	JQ957164	KC818995	JQ957446
Hemidactylus smithi	KC818715	KC818870	KC818785	KC818996	KC819055
Hemidactylus squamulatus	KC818739	KC818888		KC819005	KC819066
Hemidactylus triedrus	KF057090	HM559617	HQ426550	HM622365	HQ426466
Hemidactylus turcicus	AF363568	HQ833739	KC818793	EU268299	HQ676089
Hemidactylus ulii	KF647572		KF647577	KF647603	KF647614
Hemidactylus yerburii	KC818744	KC818898	JQ957166	KC819013	JQ957448
Hemiphyllodactylus titiwangsaensis			JQ945578	JN393978	JQ945471
Hemiphyllodactylus yunnanensis	DQ852703	FJ970983	AY172932	JN393979	JQ945472
Hemitheconyx caudicinctus	AB610502	AB610502	HQ426552	HQ426294	HQ426468
Hemitheconyx taylori	AB610503	AB610503	HQ426553	HQ426295	HQ426469
Heteronotia binoei	EF626817	EF626817	JQ945580	EU054286	JQ945473
Heteronotia planiceps			JQ945581	EU054284	JQ945474
Holodactylus africanus	AB028754		AY172933	HQ426296	HQ426470
Homonota darwinii	FJ985055	FJ985033	EU293673	EU293628	EU293718
Homonota fasciata	DQ852725	FJ985031	DQ852734	EU293629	EU293719
Homonota gaudichaudii	FJ985065	FJ985046	HQ426536	HQ426281	HQ426454
Homopholis fasciata	DQ852723		JQ945582	EU054226	JQ945475

Lepidoblepharis festae			EF564068	HQ426297	EF564094
Lepidoblepharis xanthostigma	GU139948		EU435262	EF534790	EF534957
Lepidodactylus lugubris	DQ852704		AY172934	JX515629	EF534980
Lepidodactylus novaeguineae			JQ945583	JQ945312	JQ945476
Lialis burtonis	AF090183		AY134563	EF534782	EF534948
Lucasium damaeum			AY172927	HQ426279	HQ426452
Lucasium stenodactylum			FJ855475	FJ855454	JQ945477
Luperosaurus cumingii			JQ945585	JQ945313	JQ945478
Lygodactylus arnoulti		GU593523		GU593586	GU593395
Lygodactylus bivittis		GU593542	JQ945586	JQ945314	GU593416
Lygodactylus bradfieldi	DQ852705	GU593494	AY172935	HQ426301	GU593358
Lygodactylus capensis		GU593504		KF546254	GU593372
Lygodactylus chobiensis		GU593520		KF546242	GU593390
Lygodactylus conraui		GU593502			GU593367
Lygodactylus grotei		GU593498		GU593555	GU593364
Lygodactylus guibei		GU593524		GU593588	GU593397
Lygodactylus kimhowelli		GU593535		KF546244	GU593409
Lygodactylus klugei			HQ426555	HQ426298	HQ426471
Lygodactylus lawrencei		GU593497		GU593553	GU593361
Lygodactylus luteopicturatus			FJ830142	KF546243	FJ830325
Lygodactylus miops			HQ426556	HQ426299	HQ426472
Lygodactylus mirabilis		GQ910847	HQ426557	HQ426300	GU593412
Lygodactylus mombasicus		GU593511		GU593571	GU593380
Lygodactylus stevensoni		GU593516		GU593576	GU593386
Lygodactylus tolampyae		GU593527	HQ426559	HQ426302	GU593399
Lygodactylus verticillatus		GU593528		GU593595	GU593404
Matoatoa brevipes	EU596614	EU596696	JQ945587	EF490724	JQ945480
Mediodactylus kotschyi	EU589169	EU589192		KC152030	
Mediodactylus russowii	AF323513		JQ945588	JQ945315	JQ945481
Mediodactylus spinicauda			JQ945589	KC152032	JQ945482
Microgecko helenae			JQ945590	JQ945317	JQ945483
Nactus pelagicus	DQ852706		AY172936	HM997175	JQ945484
Nactus vankampeni			JQ945591	EU054280	JQ945485
Narudasia festiva	DQ852707		AY172937	EF534808	EF534976
Naultinus gemmeus			JQ945592	GU459360	JQ945486
Nephrurus levis			JQ945593	GU459544	JQ945487
Oedodera marmorata			JQ945594	JQ173726	JQ945488
Oedura marmorata	AF090184		FJ571638	FJ571623	EF534945
Oedura tryoni	AF090179	AY583956	AF090848	JQ173757	
Ophidiocephalus taeniatus			FJ571645	FJ571630	HQ426476
Pachydactylus affinis	DQ275389	AY123414		DQ275433	
Pachydactylus austeni	DQ275371	AF449126	JQ945596	JQ945321	
Pachydactylus bicolor	DQ275394	AY123400		JN543911	
Pachydactylus capensis	DQ275387	AF449133		HQ165992	
Pachydactylus caraculicus	DQ275393	AY123399		JN543933	
Pachydactylus fasciatus	DQ275384	AF449128		HQ165979	
Pachydactylus formosus	DQ275377	AY123411		DQ275421	
Pachydactylus gaiasensis	DQ275399	AY123407	JQ945597	JN543934	JQ945490
Pachydactylus geitje	DQ275380	AF449132		JN543931	
Pachydactylus haackei	DQ275402	AF449121		DQ275446	
Pachydactylus kladaroderma	DQ275401	AF449122	JQ945598	JQ945323	JQ945491
Pachydactylus labialis	DQ275379	AF449130		DQ275423	
Pachydactylus laevigatus	AF186118	AF184990	AF363567		
Pachydactylus maculatus	DQ275382	AF449127		DQ275426	
Pachydactylus mariquensis	DQ275370	DQ278601		JN569192	
Pachydactylus namaquensis	DQ275400	AF449123		DQ275444	
Pachydactylus oculatus	DQ275381	AY123402		DQ275425	
Pachydactylus oreophilus	DQ275398	AY123406		JN543936	
Pachydactylus parascutatus	DQ275397	AY123405		JN543942	
Pachydactylus punctatus	DQ275411	AF449135	EU293691	EU293646	EU293736
Pachydactylus rangei	DQ275373	AY123397	JQ945599	JQ945324	JQ945492

Pachydactylus rugosus	DQ275376	AF449129	JQ945600	JQ945325	JQ945493
Pachydactylus sansteynae	DQ275396	AY123404		JN543940	
Pachydactylus scherzi	DQ275392	AY123401		JN543941	
Pachydactylus scutatus	DQ275395	AY123403		JN543945	
Pachydactylus serval	DQ275385	AY123409		HQ165987	
Pachydactylus tigrinus	DQ275390	AY123412		DQ275434	
Pachydactylus tsodiloensis	DQ275383	AY123408		DQ275427	
Pachydactylus vansoni	DQ275388	AY123415		DQ275432	
Pachydactylus vanzyli	DQ275372	AY123396	JQ945601	JQ945326	JQ945494
Pachydactylus weberi	DQ275386	AF449131	JQ945602	HQ165991	JQ945495
Paniegekko madjo			JQ945533	GU459549	JQ945425
Paradelma orientalis			FJ571642	FJ571626	HQ426477
Paragehyra gabriellae			JQ945603	JQ945328	JQ945496
Paroedura androyensis	GU128974	EF490748	HQ256721	EF490721	
Paroedura bastardi	GU128966		HQ256725	EF536163	
Paroedura gracilis	GU128986		HQ256726	EF536146	
Paroedura ibityensis	GU128980		HQ256729	EF536158	
Paroedura lohatsara	GU128971		HQ256731	EF536155	HE967858
Paroedura masobe	GU128977		HQ256732	EF536144	HQ426478
Paroedura oviceps	EU596615	EU596697	HQ256733	EF536159	
Paroedura picta	GU128965		EU293692	EF536149	EU293737
Paroedura sanctijohannis	HE967872			EF536157	HE967847
Paroedura stumpffi	GU128964		HQ256736	EF536154	HE967863
Paroedura vazimba	GU128981		HQ256742	EF536147	
Perochirus ateles			JQ945604	JN393984	JQ945497
Phelsuma abbotti abbotti		FJ829974	FJ830056		FJ830238
Phelsuma andamanense	AY221277	FJ829982	AY221340		FJ830246
Phelsuma antanosy		FJ829983	FJ830064		FJ830247
Phelsuma astriata	AY221273	KC347933	AY221337		KC348233
Phelsuma barbouri		FJ829988	FJ830069		FJ830252
Phelsuma berghofi		FJ829989	FJ830070		FJ830253
Phelsuma borbonica			HQ426561	HQ426305	HQ426479
Phelsuma cepediana	AY221294	AY221438	AY221360		FJ830256
Phelsuma comorensis	DQ911637	DQ911695	FJ830074		FJ830257
Phelsuma dorsivittata	KC438484	FJ830017	FJ830102		FJ830284
Phelsuma dubia	EF424452	FJ829996	FJ830076		FJ830263
Phelsuma edwardnewtoni	AY221292	AY221398	AY221353		
Phelsuma flavigularis	EF424466	FJ829998	FJ830081		FJ830265
Phelsuma gigas	AY221293	AY221399	AY221354		
Phelsuma grandis	EF424456	EF424441	AY221338		FJ830266
Phelsuma guentheri	AY221310		AY221368		FJ830267
Phelsuma guimbeaui	AY221328	HG779502	AY221372		
Phelsuma guttata	KC438513	FJ830001	FJ830085		FJ830268
Phelsuma hielscheri		FJ830002	FJ830086		FJ830269
Phelsuma inexpectata	AY221290		AY221351	JN393983	FJ830270
Phelsuma kely		FJ830004	FJ830088		FJ830271
Phelsuma klemmeri		FJ830006	FJ830090		FJ830273
Phelsuma kochi	EF424458	EF424447	AY221339		FJ830275
Phelsuma laticauda	HQ896029	HQ896029	JQ945605	JQ945329	JQ945498
Phelsuma lineata	KC438485	AY221385	AY221342		
Phelsuma madagascariensis	DQ852709	EF424449	AY172939	KF546255	FJ830290
Phelsuma modesta	EF424465	EF424451	HQ426563	HQ426307	HQ426481
Phelsuma mutabilis	AY221272	FJ830027	AY221336		FJ830295
Phelsuma nigristriata		FJ830032	FJ830117		FJ830300
Phelsuma ornata	AY221312		AY221369		FJ830301
Phelsuma parkeri	DQ911693	DQ911751			FJ830302
Phelsuma parva		FJ830037	FJ830125		FJ830308
Phelsuma pasteuri	DQ911691	DQ911749	FJ830120		FJ830303
Phelsuma pronki		FJ830034	FJ830121		FJ830304
Phelsuma pusilla	KC438509	FJ830035	FJ830122		
Phelsuma quadriocellata	AY221282	FJ830036	AY221345		FJ830306

Phelsuma robertmertensi	DQ911642	DQ911701	FJ830128		FJ830311
Phelsuma rosagularis	AY221324	FJ830041	HQ426562	HQ426306	FJ830312
Phelsuma seippi		FJ830042	FJ830130	KF546256	FJ830313
Phelsuma serraticauda	AY221278		AY221341		FJ830314
Phelsuma standingi	AY221281	AY221387	AY221344	GU593610	FJ830316
Phelsuma vanheygeni		FJ830049	FJ830137		FJ830320
Phelsuma vnigra	DQ911674	DQ911734	FJ830138		FJ830321
Phyllodactylus bordai			HQ426565	HQ426309	HQ426483
Phyllodactylus bugastrolepis			EU293676	EU293631	EU293721
Phyllodactylus delcampoi			HQ426566	HQ426310	HQ426484
Phyllodactylus homolepidurus			JQ945606	JQ945330	JQ945499
Phyllodactylus kofordi			JQ821736	JQ821794	JQ821761
Phyllodactylus nocticolus	FJ662576		FJ662515	HQ426311	HQ426485
Phyllodactylus reissii	JQ821788		JQ821741	EU293632	JQ821763
Phyllodactylus tuberculosus			EU293675	EU293630	EU293720
Phyllodactylus unctus	HQ896027	HQ896027	FJ662502	HQ426312	HQ426486
Phyllodactylus wirshingi			JQ945607	JQ945331	JQ945500
Phyllodactylus xanti	FJ662569		FJ662506	EF534807	EF534975
Phyllopezus lutzae			HQ426522	JN935431	HQ426438
Phyllopezus maranjonensis		JQ826820	JN935479	JN935437	EU293723
Phyllopezus periosus		JQ826832	JN935475	JN935434	JN935405
Phyllopezus pollicaris	DQ852721	JQ826844	JN935477	JN935466	JN935424
Phyllurus platurus			AY172941	FJ855443	HQ426488
Pletholax gracilis			AY134566	FJ571631	HQ426489
*Pristurus sp.*1	KJ849893		KJ850011	KJ850084	KJ850157
Pristurus abdelkuri	KJ849839		KJ849973	KJ850033	KJ850108
Pristurus adrarensis	KJ849842		KJ849975	KJ850035	KJ850110
Pristurus carteri	KJ849849		KJ849981	KJ850042	KJ850117
Pristurus celerrimus	KJ849854		KJ849984	KJ850047	KJ850722
Pristurus collaris	KJ849858			KJ850049	KJ850124
Pristurus crucifer	KJ849860		KJ849987	KJ850051	KJ850126
Pristurus flavipunctatus	KJ849865		KJ849991	KJ850056	KJ850130
Pristurus gallagheri	KJ849875		KJ849996	KJ850065	KJ850138
Pristurus guichardi	KJ849877		KJ849997	KJ850067	KJ850140
Pristurus insignis	KJ849878		KJ849998	KJ850068	KJ850141
Pristurus insignoides	KJ849880		KJ850000	KJ850070	KJ850143
Pristurus minimus	KJ849881		KJ850001	KJ850071	KJ850144
Pristurus obsti	KJ849886		KJ850006	KJ850076	KJ850149
Pristurus popovi	KJ849887			KJ850077	KJ850150
Pristurus r. rupestris 1	KY023457	KY023856	KY023908	KY024045	KY024118
Pristurus r. rupestris 10.11	KY023386	KY023829	KY023920	KY024038	KY024111
Pristurus r. rupestris 12	KY023396	KY023832	KY023932	KY024074	KY024144
Pristurus r. rupestris 13	KY023407	KY023839	KY023923	KY024078	KY024147
Pristurus r. rupestris 14	KY023418	KY023835	KY023936	KY024080	KY024149
Pristurus r. rupestris 15	KY023441	KY023845	KY023937	KY024085	KY024154
Pristurus r. rupestris 16	KY023453	KY023855	KY023953	KY024044	KY024117
Pristurus r. rupestris 2	KY023478	KY023860	KY023905	KY024086	KY024155
Pristurus r. rupestris 3	KY023590	KY023873	KY023914	KY024056	KY024126
Pristurus r. rupestris 4.5	KY023671	KY023869	KY023904	KY024068	KY024138
Pristurus r. rupestris 6	KY023687	KY023847	KY023954	KY024089	KY024157
Pristurus r. rupestris 7	KY023742	KY023853	KY023961	KY024095	KY024163
Pristurus r. rupestris 8	KY023759	KY023878	KY023946	KY024099	KY024167
Pristurus r. rupestris 9	KY023786	KY023879	KY023947	KY024101	KY024169
Pristurus samhaensis	KJ849910		KJ850025	KJ850101	KJ850173
Pristurus sokotranus	KJ849913		KJ850028	KJ850104	KJ850176
Pristurus somalicus	KJ849916		KJ850032	KJ850107	KJ850180
Pseudoceramodactylus khobarensis	KC190704		KC191004		KC191124
Pseudogekko smaragdinus			JQ945608	JQ945332	JQ945501
Pseudogonatodes guianensis			EU435260	HQ426317	HQ426490
Pseudothecadactylus lindneri	AF090177		AF090846	AY662626	HQ426492
Ptenopus carpi	DQ852711		AY172942	JQ945333	JQ945502

Ptychozoon kuhli			JQ945610	JQ945334	JQ945503
Ptychozoon lionotum			JQ945611	JX515640	JQ945504
Ptyodactylus guttatus			EU293681	EU293636	EU293726
Ptyodactylus hasselquistii	GU195735		EU293682	EU293637	EU293727
Pygopus lepidopodus			FJ571643	FJ571627	HQ426493
Pygopus nigriceps	DQ852693		FJ571644	FJ571628	EF534949
Quedenfeldtia moerens	JQ686302		HQ426574	HQ426320	HQ426494
Quedenfeldtia trachyblepharus	JQ686294		EF534930	EF534804	EF534972
Rhacodactylus ciliatus			EF534902	JX024482	EF534944
Rhacodactylus leachianus	AF090176		FJ855467	JX024552	JQ945505
Rhoptropella ocellata	AY221271	EU596700	AY221335	HQ426308	FJ830324
Rhoptropus afer	DQ275409	AY026923	JQ945613	JQ945336	JQ945506
Rhoptropus boultoni	DQ852712	AY221375	AY221333	DQ275454	EF534978
Rhoptropus bradfieldi diporus	EU596606	EU596690	JQ945614	JQ945337	JQ945507
Rhynchoedura ornata	AF090181		FJ855476	JX024563	JQ945508
Saltuarius swaini		EU625323	JF807316	FJ855444	JQ945509
Saurodactylus brosseti	EU014307		HQ426575	HQ426321	EF534970
Saurodactylus fasciatus	EU014296		HQ426576	HQ426322	HQ426495
Saurodactylus mauritanicus	GU139953		GU139846	HQ426323	HQ426496
Sphaerodactylus argus			HQ426578	HQ426324	HQ426497
Sphaerodactylus elegans			EF534912	EF534787	EF534954
Sphaerodactylus glaucus			HQ426579	HQ426325	HQ426498
Sphaerodactylus klauberi	KC840434		HQ426581	HQ426327	HQ426500
Sphaerodactylus macrolepis			HQ426580	HQ426326	HQ426499
Sphaerodactylus nicholsi	KC840508		HQ426582	HQ426328	HQ426501
Sphaerodactylus nigropunctatus			EF534911	HQ426329	EF534953
Sphaerodactylus notatus			EF564067	HQ426330	EF564093
Sphaerodactylus ocoae			EF534910	EF534786	EF534952
Sphaerodactylus roosevelti	DQ852713		AY172946	EF534785	EF534951
Sphaerodactylus torrei			EF534913	EF534788	EF534955
Sphaerodactylus townsendi	KC840514		HQ426583	HQ426331	HQ426502
Stenodactylus affinis	KC190679		KC190945		KC191056
Stenodactylus arabicus	KF898413		KC190999		KC191116
Stenodactylus doriae	KC190652		KC190938	KC152037	KC191046
Stenodactylus grandiceps	KC190667		KC190951		KC191135
Stenodactylus leptocosymbotes	KC190663		KC190942		KC191052
Stenodactylus mauritanicus	KC190601		KC191008		KC191080
Stenodactylus petrii	DQ852722		KC191007	JX440679	KC191095
Stenodactylus pulcher	KC190701		KC191002		KC191120
Stenodactylus slevini	KC190687		KC190948		KC191057
Stenodactylus sthenodactylus	KC190524		KC190968	JQ945339	KC191082
Stenodactylus yemenensis	KC190717		KC191029		KC191064
Strophurus ciliaris	AY583857	AY583942		JQ173762	
Strophurus elderi			JQ945618	JQ173763	JQ945512
Strophurus intermedius	AF090180		AF039469	FJ571625	
Strophurus strophurus			JQ945619	JQ173766	JQ945513
Tarentola americana	AF186119	AF184991	AF363542	HQ426332	HQ426503
Tarentola angustimentalis	AF186120	AF184994	AF363546		JQ301379
Tarentola annularis	AF363571	AF364322	AF363552	DQ275456	JQ301432
Tarentola boehmei	AF363569	AF364320	AF363543		JQ301427
Tarentola boettgeri	Z93327	AY841914	AF315387		
Tarentola chazaliae	AF363574	AF364325	AF363556	EU293638	JQ301343
Tarentola delalandii	AF186129	AF185001	KC191034	EU293639	KC191144
Tarentola deserti	AF363570	AF364321	AF363544	HQ426333	JQ301411
Tarentola ephippiata	AF363572	AF364323			JQ301364
Tarentola fascicularis	JQ300757			HQ426334	JQ301435
Tarentola gigas	AF468807		AF363563	EU293640	EU293730
Tarentola mauritanica	EU443255	JQ425057	AF363566	EU293641	HM014737
Tenuidactylus caspius	EU589164		JQ945620	JQ945340	JQ945514
Tenuidactylus elongatus	AF323512		AY172925	JX440677	
Tenuidactylus longipes	EU589170	EU589193	JQ945621	JQ945341	JQ945515

Teratoscincus keyserlingii	AY753545	AY753545	HQ426589		HQ426508
Teratoscincus microlepis	KC190728		KC191041	EF534800	KC191151
Teratoscincus przewalskii			AY172947	AY662624	HQ426507
Teratoscincus roborowskii	DQ852714		KC191040	EF534799	KC191150
Teratoscincus scincus	KC190726	KF258129	KC191039	HM161239	KC191149
Thecadactylus rapicauda			EU293687	EU293643	EU293733
Thecadactylus solimoensis			EU293689	EU293644	EU293734
Tropiocolotes algericus	KC190710		KC191023		KC191129
Tropiocolotes nubicus	KC190706		KC191021	KC152042	KC191126
Tropiocolotes scortecci	KC190707		KC191022		KC191127
Tropiocolotes steudneri	DQ852727		KC191020	JX440680	KC191125
Tropiocolotes tripolitanus	KC190712		KC191024	JQ945343	KC191130
Underwoodisaurus milii	AF090174	GQ865777	FJ571637	FJ571622	EF534946
Urocotyledon inexpectata		JN225790	JQ945624	JQ945344	JN225815
Uroplatus alluaudi	EU596620	EU596701		EF490740	
Uroplatus ebenaui	EU596623	EU596703	JN038089	EF490734	
Uroplatus fimbriatus	EU596644	EU596723		EF490739	
Uroplatus giganteus		EF490765	JQ945625	EF490738	JQ945519
Uroplatus guentheri	EU596689	EU596764	JQ945626	EF490725	JQ945520
Uroplatus henkeli	EU596651	EU596729	HQ426591	EF490743	HQ426510
Uroplatus lineatus	EU596658	EU596734		EF490727	HE967860
Uroplatus phantasticus	EU596667	EU596747	JN038075	EF490746	HQ426511
Uroplatus pietschmanni	EU596687	EU596763		EF490728	
Uroplatus sikorae	EU596672	EU596749		EF490731	
Uvidicolus sphyrurus		GQ865776	JQ945627	GU459543	JQ945521
Woodworthia maculatus			JQ945628	GU459443	JQ945522

Table S3. Measurements (in millimetres) of the 155 specimens of *Pristurus rupestris rupestris* used in the morphological differentiation analysis. Abbreviations: Snout vent length (SVL), head length (HL), head width (HW), head depth (HD), amplitude of the scapular girdle (ASG), amplitude of the pelvic girdle (APG), axilla-groin length (AGL), brachium length (BL), antebrachium length (AL), thigh length (TL) and crus length (CL). Candidate species refer to the candidate species recognized by the BP&P analysis of dataset 2. For information on the geographical localities of the different specimens see Table S1.

Candidate species	Specimen code	SVL	HL	HW	HD	ASG	APG	AGL	BL	AL	TL	CL
1	S6064	25.81	6.52	4.49	3.12	3.94	3.94	9.32	4.9	4.61	6.9	6.22
1	S6134	23.75	6.26	4.44	3.42	4.08	3.67	9.93	4.36	4.14	5.66	5.42
1	S7809	22.2	5.88	3.79	2.65	2.86	2.89	9.05	2.88	3.54	5.09	4.7
1	CN190	25.41	6.19	4.42	3.1	4.13	3.48	11.29	3.85	4.23	5.18	6.03
1	CN4018	26.15	6.57	4.49	3.47	4.38	4.09	10.96	3.72	4.78	5.7	6.44
1	CN4246	25.7	6.69	4.63	3.21	4.29	3.55	10.48	3.74	4.87	5.42	5.84
2	S6124	25.8	6.38	4.44	3.2	4.15	3.59	10.02	4	4.64	5.98	6.3
2	S7239	23.75	5.98	4.4	2.92	3.88	3.16	9.36	3.49	3.24	5.51	5.31
2	S7245	24.63	6.3	4.28	2.89	4.02	3.54	9.62	3.75	4.64	6.14	5.79
2	S7273	25.37	6.35	4.36	3.02	3.97	3.25	10.14	3.19	4.26	5.53	6.12
2	S7489	24.94	6.26	4.17	3.09	3.81	3.52	9.02	3.33	4.1	5.38	5.42
2	S7702	24.81	6.44	4.75	3.54	3.91	3.77	10.35	4.15	5.36	6.08	6.86
2	CN4237	24.27	5.93	4.1	2.89	4	3.05	10.25	3.92	4.33	5.37	6.05
2	CN6975	24.42	6.05	4.4	2.98	4.33	3.44	10.12	4.07	4.33	5.19	5.42
3	S1673	26.03	6.15	5.14	3.03	3.68	3.62	10.78	4.08	4.64	5.21	5.89
3	S1689	26.1	6.55	4.35	3.05	3.43	3.36	7.72	4.45	4.74	5.35	5.92
3	S1773	23.56	6.04	4.18	3.03	3.52	3.28	9.16	3.6	4.08	5.96	5.53
3	S1799	24.23	5.91	4.32	3.2	3.61	3.6	9.98	3.49	4.03	5.68	5.48
3	S6100	26.47	6.5	4.9	3.3	4.2	3.7	11.73	4.57	5.01	6.14	6.65
3	S7247	23.07	5.69	4.11	2.91	3.88	3.05	9.21	3.5	4.35	5.74	4.91
3	S7409	25.27	6.16	4.16	3.09	3.29	3.49	9.96	3.99	4.35	5.51	5.63
3	S7457	22.97	5.84	4.27	2.98	3.04	3.04	9.8	2.94	3.75	5.17	5.05
3	S7525	26.29	6.8	4.47	3.18	4.85	4.01	10.88	3.74	4.2	5.94	6.2
3	S7534	24.51	6.24	4.55	3.08	4.14	3.79	10.29	4.07	4.7	5.66	5.87
3	S7544	26.13	6.65	4.41	3.11	3.75	3.4	10.35	4.49	4.21	5.71	5.89
3	S7553	25.34	6.31	4.38	2.93	4.08	3.84	9.88	4.33	4.76	5.63	5.99
3	S7561	24	6.22	4.15	2.91	3.47	3.33	9.97	3.64	4.29	5.08	5.42
3	S7709	25.63	6.67	4.54	3.31	4.2	3.59	10.09	3.89	4.85	5.75	6.39
3	S9016	23.52	5.98	4.3	3.39	3.67	3.12	9.19	3.68	4.52	5.08	5.98
3	S9018	25.7	6.55	4.73	3.36	4.8	3.97	10.19	4.21	4.68	5.48	6.49
3	CN179	27.37	6.77	4.75	3.5	3.71	3.39	12.19	4.08	4.92	5.81	5.91
3	CN3705	24.42	6.19	4.22	3.2	3.89	3.13	10.29	3.7	4.39	5.35	5.85
3	CN3720	25.56	6.47	4.53	3.2	3.8	3.09	11.05	4.1	4.59	5.43	5.88
3	CN3997	25.5	6.59	4.42	3.47	3.59	3.29	9.68	3.66	4.57	5.39	5.56
3	CN4175	24.51	5.94	4.4	3.14	4.02	3.19	10.23	3.58	4.17	4.92	5.74
3	CN7147	24.13	6.29	4.24	2.89	4.11	3.14	10.65	3.66	4.26	4.67	5.32
3	CN8972	25.62	6.2	4.27	3.25	3.91	3.4	10.72	3.68	4.37	4.88	5.79
3	UAE58	24.42	6.21	4.23	2.92	3.42	3.39	9.51	3.81	3.5	6.38	5.57
4.5	S6116	26.01	6.8	4.75	3.09	4.06	3.65	10.69	3.69	4.96	4.97	5.56
4.5	S6132	27.01	7.04	5.01	3.82	3.96	4.06	9.74	4.4	4.21	6	6.81
4.5	S7158	25.18	6.34	4.52	3.94	3.9	3.49	10.39	4.32	3.78	5.05	6.45
4.5	S7159b	22.41	5.84	4.58	3.25	4.37	3.57	8.8	3.56	4.24	5.38	5.26
4.5	S7196	24.19	6.07	4.34	3.28	3.86	3.66	10.45	4.62	4.27	5.33	4.94
4.5	S7209	23.9	5.92	4.28	3.1	3.6	3.14	9.42	3.52	4.13	4.98	5.08
4.5	S7233	26.44	6.4	4.74	3.22	3.88	3.64	11.35	3.48	4.27	5.29	6.04
4.5	S7249	23.71	5.98	4.46	2.74	3.17	3.56	9.64	4.11	4.35	5.13	5.05
4.5	S7251	24.52	6.3	3.94	2.99	3.48	3.16	9.85	3.36	4.77	5.47	5.13
4.5	S7255	21.5	5.51	3.95	2.87	3.04	3.19	7.88	2.96	3.69	4.88	4.89
4.5	S7433	24.37	5.96	4.29	2.97	3.84	3.08	10.09	3.48	4.11	4.75	5.98
4.5	S7440	26.33	6.11	4.52	3.33	3.79	3.77	9.45	4.42	4.41	4.96	5.81
4.5	S7461	25.88	6.46	4.88	3.45	4.41	4	11.19	3.68	4.86	4.1	6.24
4.5	S7462	25.21	6.78	4.92	3.86	4.67	3.94	10.76	4.84	4.79	5.41	6.02

4.5	CN32	25.22	6.15	4.63	3.05	4.13	3.36	11.59	4.06	4.19	5.05	5.4
4.5	CN3424	26.7	6.44	4.34	3.13	3.76	3.5	12.21	4.42	4.41	5.02	5.7
4.5	CN3709	26.04	6.46	4.42	3.27	4.03	3.46	10.67	4.25	4.44	5.44	5.34
4.5	CN5829	23.95	5.88	4.29	2.81	3.66	3.15	10.13	3.72	3.93	4.85	4.96
6	S7185	23.87	6.67	4.83	4.1	3.99	3.37	10.03	4.81	4.43	4.45	6.3
6	S7198	25.91	6.44	4.81	3.39	4.1	4.09	10.96	3.8	4.27	4.91	5.19
6	S7201b	24.92	6.47	4.77	3.45	3.84	3.87	10.05	3.86	4.69	5.6	5.63
6	S7203	23.82	6.51	4.78	3.92	4.23	4.31	8.55	3.8	4.22	5.33	5.59
6	S7216	24.44	6.78	4.97	3.52	3.52	3.4	9.03	3.33	4.46	5.53	5.44
6	S7231	25.68	6.48	5.17	3.94	4.58	4.37	11.19	4.16	4.09	5.83	6.17
6	S7259	24.34	6.31	4.79	3.44	4.36	4.1	9.52	3.86	4.72	5.79	5.57
6	S7507	25.61	6.45	4.74	3.41	4.07	3.7	10.09	3.26	4.43	5.54	5.49
6	S7570	22.97	6.33	4.77	3.35	4.05	3.49	8.98	3.35	4.08	5.08	5.64
6	CN3737	25.46	6.62	4.79	3.61	4.23	3.77	10.22	3.69	4.46	5.62	5.34
6	CN6980	26.08	6.9	5.09	3.66	3.81	3.77	10.68	3.42	4.64	5.41	6.27
6	CN7096	23.22	6.15	4.43	3.27	4.02	3.3	9.98	3.67	4.41	4.93	5.19
6	CN7112	25.8	6.71	4.63	3.7	4.05	3.47	11.06	3.77	4.15	5.23	5.87
6	CN7168	25.35	6.63	4.76	3.53	3.78	3.54	11.29	3.8	4.01	5.33	5.04
6	CN7181	23.99	6.07	4.62	3.45	4.01	3.38	9.68	3.71	4.27	5.04	5.16
6	CN7215	25.03	6.67	4.55	3.52	4.43	3.58	10.58	3.69	4.32	4.93	5.8
6	CN7960	25.29	6.63	4.96	3.63	4.08	3.23	10.92	3.97	4.44	5.47	5.58
7	S7264	26.14	6.57	4.9	3.41	4.04	3.61	10.4	3.57	4.14	5.68	5.51
7	S7486	25.09	6.32	4.56	3.23	4.42	3.66	9.4	3.45	4.42	5.39	5.61
7	S7510	25.38	6.19	4.31	3.07	3.72	3.6	10.01	3.42	4.44	5.17	5.03
7	S7511	24.92	6.58	4.8	3.4	4.03	3.95	9.32	3.35	4.64	6.36	5.43
7	S7529	25.4	6.73	5.6	3.58	4.63	3.64	10.4	3.53	4.65	6.19	6.23
7	S7531	24.66	6.7	5.52	3.45	4.83	4.19	9.66	3.74	4.48	5.45	5.68
7	S7539	25.41	6.69	4.91	3.32	4.33	4.11	10.14	4.23	3.91	4.97	5.29
7	S7547	24.79	6.69	4.6	3.45	4.09	3.56	8.46	3.85	4.4	6.27	5.77
7	S7556	25.55	6.68	4.97	3.37	3.9	3.75	10.09	3.39	4.98	5.83	5.78
7	S7560	24.83	6.72	4.75	3.17	3.99	3.48	8.72	3.62	3.7	5.68	5.29
7	CN127	24.28	6.21	4.51	3.46	3.66	3.5	9	3.02	3.89	4.92	5.35
7	CN175	25.72	6.89	4.86	3.75	4.2	3.92	10.4	3.8	4.52	5.49	6.28
7	CN3480	25.57	6.66	4.88	3.7	3.88	3.53	11.07	3.41	3.63	4.73	5.37
7	CN3491	25.11	6.72	5.24	3.56	3.81	3.67	10.31	3.17	4.89	4.98	5.32
7	CN3507	26.86	7.04	5.29	3.74	4.46	3.69	10.46	3.72	4.6	5.42	6.04
7	CN4165	25.51	6.55	4.52	3.41	4.36	3.37	9.78	3.52	4.34	4.73	5.83
7	CN4188	26.4	7.02	5.03	3.61	4.64	3.69	11.16	3.83	4.55	5.18	5.97
7	CN7212	26.87	6.67	4.79	3.58	4.13	3.88	11.04	3.61	4.43	5.27	5.79
7	CN7269	23.45	6.35	4.34	3.35	4.04	2.87	8.74	3.47	3.99	4.68	4.89
7	CN8286	24.54	6.72	4.9	3.58	4.38	3.89	10.37	3.74	4.52	5.45	6.07
8	S7508	22.93	5.68	4.11	2.99	3.81	3.65	9.06	3.58	3.66	5.5	5.17
8	S7577	22.02	6	4.01	3.21	3.52	3.12	8.32	3.5	4.03	5.01	4.88
8	S8000	22.35	5.8	4.32	3.34	3.91	3.44	10.11	3.28	4.85	5.42	5.21
8	CN159	22.73	6.05	4.25	3.32	3.5	3.13	7.6	3.41	3.96	4.52	5.25
8	CN3588	19.96	5.47	3.93	3.09	3.19	2.9	7.54	3.22	3.69	4.15	5.18
8	CN7971	21.41	5.85	3.99	3.03	3.88	3.27	8.26	3.23	3.84	4.71	5.06
8	CN8037	21.06	5.66	3.9	2.98	3.36	2.56	8.64	3.3	3.73	4.36	4.52
8	CN8965	21.87	5.76	4.03	3.21	3.28	2.96	8.82	3.55	3.71	4.57	4.87
9	S1645	23.63	5.84	4.09	2.76	3.05	3.05	9.46	3.33	3.86	5.15	5.02
9	S1891	24	6.22	4.32	2.98	3.58	3.53	9.5	3.51	4.93	5.75	4.61
9	S7276	24.86	6.1	4.23	3.22	3.87	3.06	9.73	4.82	4.06	5.42	5.91
9	S7437	22.27	5.77	4.07	2.92	3.18	3	8.57	2.86	3.82	4.82	5.2
9	S7541	25.79	6.86	4.7	3.25	4.42	3.58	9.04	5.16	5.81	6.23	5.86
9	S7865	23.16	6.26	4.72	3.75	3.83	3.4	10.11	4.03	3.61	5.25	4.96
9	S9012	23.2	6.54	4.3	3.24	3.79	3.19	9.19	3.66	4.44	5.04	5.68
9	S9013	23.23	6.14	4.3	3.23	3.79	3.53	8.58	3.85	3.8	5.31	5.38
9	CN145	23.1	5.64	3.87	3.17	3.44	3.34	10.15	3.26	3.83	4.6	5.06
9	CN4023	23.68	6.01	4.3	3.41	3.7	3.33	9.9	3.62	3.88	5.11	5.46
10.11	S7166	24.11	6.21	4.69	3.2	3.42	3.44	9.71	3.86	4.28	5.11	5.36
10.11	S7167b	24.91	6.8	4.68	3.77	4.25	3.77	10.51	4.36	4.41	5.17	6.04

10.11	S7407	26.49	6.59	5.12	3.91	4.17	3.7	11.7	4.2	4.39	5.29	6.51
10.11	S7415	24.57	6.23	4.42	3.3	3.65	3.77	11.18	4.75	3.89	6.38	5.57
10.11	S7459	24.3	6.1	4.63	3.13	3.35	3.28	10	3.35	4.13	4.95	5.44
10.11	S7882	25.82	6.71	4.86	3.76	4.03	3.76	10.6	4.3	4.63	5.4	6.15
10.11	CN4244	24.42	5.94	4.13	2.64	3.32	2.95	10.2	3.42	3.86	5.24	4.95
10.11	CN8298	26.68	6.61	4.46	3.46	4.66	3.87	11.53	3.63	4.28	4.93	5.73
10.11	UAE31	24.39	6.21	4.41	2.93	3.48	2.92	9.1	3.41	4.17	4.95	5.14
10.11	UAE34	22.79	5.88	3.86	2.77	3.23	3.18	8.06	3.75	3.76	5.43	4.2
10.11	UAE40	25.78	6.19	4.47	3.09	3.39	3.8	9.86	3.8	4.1	4.97	5.16
12	S6060	24.94	6.52	4.86	3.39	4.18	3.87	10.25	4.25	4.02	4.76	5.2
12	S7120	22.45	6.17	4.25	2.94	4.08	3.38	9.37	4.4	4.57	5.66	5.22
12	S7452	22.45	5.71	4.2	3.41	3.71	3.5	8.44	3.59	3.76	5.08	4.66
12	S7475	25.34	6.48	4.84	3.15	4.02	3.92	10.31	3.62	4.27	5.7	6
12	S7730	20.94	5.58	4.02	3.33	3.65	3	7.9	3.24	4.05	4.47	5.2
12	CN39	24.6	6.43	4.41	3.05	3.87	3.43	10.69	3.78	4.27	5.21	5.78
12	CN4171	25.97	6.45	4.51	3.24	4.2	3.49	11.01	3.81	4.36	5.32	5.29
13	S6102	25.39	6.51	4.34	3.24	3.76	3.54	10.66	4.2	5.49	5.77	5.55
13	S6123	24.84	6.57	4.56	3.12	4.02	3.74	9.45	3.38	4.96	5.67	5.73
13	S7526	25.48	6.73	4.48	3.21	3.94	3.56	9.11	4.2	4.48	5.58	5.89
13	S7533	24.7	7.05	4.45	3.13	3.67	3.13	9.86	4.47	4.86	6.41	6.47
13	S7551	24.22	6.37	4.46	3.13	4.22	3.74	9.87	4.14	4.52	5.18	5.3
13	CN3489	26.76	6.64	4.54	3.2	4.35	3.46	10.22	4.14	4.94	5.79	6.15
13	CN3699	24.98	6.35	4.42	3.11	4.38	3.47	11.2	3.78	4.51	5.74	6.33
13	CN7239	25.26	6.37	4.49	2.99	3.67	3.13	10.91	3.43	4.3	5.51	5.49
14	S7312	24.77	6.59	4.8	3.24	4.3	3.39	8.84	3.07	3.92	6.01	5.51
14	S7528	25.19	6.44	4.95	3.3	3.98	3.79	9.87	4.11	3.9	5.62	5.42
14	S7736	25.54	6.68	5.26	3.44	3.9	4.03	10.89	3.82	4.55	4.6	5.93
14	CN4174	24.35	5.97	4.49	2.95	4.53	3.19	10.6	3.79	3.95	5.73	5.3
14	CN7200	24.4	6.29	4.66	3.22	4.51	3.17	10.6	3.93	4.55	5.39	5.33
15	S6122	26.78	6.34	4.81	3.18	3.95	4.01	10.72	4.64	4.51	6.19	6.15
15	S7258	26.39	6.68	4.57	3.23	3.92	3.62	10.3	3.38	4.53	5.4	5.85
15	S7546	27.18	6.57	4.83	3.21	4.27	3.77	10.76	3.89	4.34	6.01	5.74
15	S7644	25.26	6.49	4.73	3.56	4.05	4.21	9.54	3.77	4.46	5.31	6.52
15	S7989	25.18	6.25	4.46	3.06	3.83	3.54	10.08	3.54	4.32	5.24	5.53
15	CN3717	26.44	6.67	4.42	3.21	4.41	3.32	11.48	3.52	4.51	5.42	5.66
15	CN8031	23.89	5.96	4.4	3.15	4.37	3.26	9.24	3.93	4.16	5.07	5.89
15	CN8289	25.88	6.49	4.42	3.45	3.88	3.67	10.7	4.19	4.69	5.47	6.09
15	CN8662	25.75	6.25	4.5	3.27	4.36	3.6	11.09	4.06	4.52	5.39	5.89
15	UAE44	26.61	6.32	4.57	3.27	3.47	3.46	10.15	4.36	4.48	5.88	5.75
15	UAE45	27.36	6.48	4.8	3.28	4.34	3.58	11.39	4.61	4.71	5.7	6.09
16	S7257	23.96	6.36	4.71	3.07	4.65	4.13	10.11	3.4	3.62	5.45	5.11
16	CN3704	23.23	6.15	4.35	3.06	3.74	3.16	10.08	3.61	3.87	4.62	5.1

Table S4. Lower-left, uncorrected *p*-distances for the *12S* mitochondrial gene fragment among all 14 candidate species of *P. rupestris rupestris* inferred using dataset 1. Upper-right, standard error estimates.

	1	**2**	**3**	**4.5**	**6**	**7**	**8**	**9**	**10.11**	**12**	**13**	**14**	**15**	**16**
1		0.008	0.011	0.015	0.016	0.017	0.021	0.021	0.018	0.018	0.018	0.017	0.018	0.017
2	0.029		0.010	0.014	0.016	0.017	0.021	0.021	0.017	0.017	0.017	0.017	0.017	0.016
3	0.050	0.052		0.013	0.016	0.016	0.021	0.021	0.017	0.018	0.018	0.017	0.018	0.016
4.5	0.082	0.075	0.064		0.016	0.015	0.020	0.021	0.017	0.018	0.017	0.017	0.017	0.016
6	0.092	0.094	0.088	0.114		0.008	0.018	0.020	0.016	0.016	0.016	0.015	0.015	0.016
7	0.106	0.103	0.093	0.113	0.028		0.018	0.020	0.015	0.016	0.017	0.015	0.014	0.015
8	0.182	0.181	0.172	0.198	0.159	0.159		0.015	0.019	0.020	0.021	0.019	0.019	0.020
9	0.193	0.189	0.180	0.209	0.174	0.176	0.085		0.020	0.021	0.021	0.020	0.020	0.021
10.11	0.153	0.141	0.143	0.171	0.137	0.129	0.195	0.200		0.010	0.014	0.012	0.013	0.017
12	0.144	0.135	0.138	0.163	0.129	0.121	0.204	0.203	0.064		0.014	0.013	0.013	0.017
13	0.146	0.135	0.146	0.163	0.138	0.132	0.207	0.210	0.110	0.096		0.013	0.014	0.017
14	0.127	0.121	0.123	0.142	0.114	0.106	0.193	0.180	0.085	0.079	0.081		0.011	0.017
15	0.122	0.116	0.124	0.150	0.106	0.096	0.183	0.179	0.094	0.088	0.097	0.052		0.016
16	0.111	0.102	0.092	0.117	0.115	0.117	0.188	0.199	0.151	0.152	0.146	0.130	0.121	

Table S5. Information on the 12 localities out of a total of 233 (5.1%) in which different candidate species of *Pristurus rupestris rupestris* were found in sympatry when a buffer of 100 meters was applied. Despite the through sampling, a maximum of two different candidate species was found in sympatry in a given buffer. The number of specimens found in sympatry varied among localities. For a correlation between specimen codes and candidate species see Table S1.

Latitude	Longitude	Candidate species	Specimen codes
22.5390	59.3682	3 and 9	S7310, S9013
22.7111	59.1412	6 and 7	S7186b, S7188, S7211, S7226, S7229, S7231, S7756
22.7625	58.8531	3 and 9	S7552, S7565
22.7662	59.0337	15 and 7	S7258, S7511, S7547
22.7703	59.0758	15 and 7	S7546, S7560
22.8333	58.9882	3 and 9	S7541, S9018
22.8469	59.1381	3 and 7	CN127, CN179
22.9088	59.1715	3 and 8	S7187, S7536, CN3705
22.9819	57.7006	1 and 14	S6120, S7284
23.0799	57.6130	1 and 14	S6035, S6036, S6101
23.1317	58.6189	3 and 16	S7257, S7534, S7553, CN169, CN176, CN192, CN212, CN3704, CN4044, CN4048, CN4052, CN4175, CN6997, CN7147, CN7171, CN7208, CN7282, CN8046, CN8653, CN8956, CN8972, CN8983, CN98
23.1397	57.8442	9 and 12	S6060, S7452, S7460, S7475

Table S6. Loadings, eigenvalues, and variance explained by each of the first eight components retained from the PCA performed on shape residuals of *Pristurus rupestris rupestris*. Abbreviations of each variable as in Table S3.

Variable	PC1	PC2	PC3	PC4	PC5	PC6	PC7	PC8
HL	-0.7044	-0.0358	0.3185	0.3099	-0.0506	0.2398	-0.3284	0.1702
HW	-0.7700	-0.3428	0.1546	-0.0656	-0.0870	0.0940	-0.0940	-0.1782
HD	-0.7589	-0.3351	0.0095	0.1324	0.3209	0.0365	-0.0617	-0.1257
ASG	-0.6757	-0.0754	-0.2396	-0.2097	-0.2683	-0.1787	0.1044	0.5585
APG	-0.6618	-0.0468	0.1546	-0.5039	-0.0401	-0.0467	0.3828	-0.2465
AGL	-0.0048	-0.3403	-0.7968	-0.1207	-0.3020	0.0838	-0.2794	-0.2083
BL	-0.2838	0.5068	-0.4226	-0.2425	0.5114	0.3763	-0.0063	0.1068
AL	-0.3695	0.5158	-0.1627	0.4556	-0.3996	0.2682	0.3250	-0.1313
TL	-0.1599	0.7066	0.2539	-0.3807	-0.2455	-0.0886	-0.3979	-0.1168
CL	-0.5264	0.3412	-0.2808	0.3208	0.2093	-0.5876	-0.0506	-0.1208
Eigenvalue	3.08	1.49	1.19	0.94	0.80	0.68	0.62	0.55
Variance explained (%)	30.79	14.93	11.90	9.45	8.03	6.75	6.23	5.49

Table S7. Assignation of each of the specimen of *Pristurus rupestris rupestris* measured to the most probable candidate species according to the linear discriminant function analysis (DFA) of the 155 specimens from Table S3. For information on the geographical locality of the different specimens used see Table S1.

Specimen code	Candidate species	DFA classification
S6064	1	2
S6134	1	12
S7809	1	9
CN190	1	2
CN4018	1	15
CN4246	1	13
S6124	2	2
S7239	2	14
S7245	2	13
S7273	2	2
S7489	2	15
S7702	2	3
CN4237	2	2
CN6975	2	4.5
S1673	3	4.5
S1689	3	15
S1773	3	1
S1799	3	1
S6100	3	15
S7247	3	9
S7409	3	3
S7457	3	10.11
S7525	3	1
S7534	3	1
S7544	3	1
S7553	3	1
S7561	3	1
S7709	3	13
S9016	3	9
S9018	3	2
CN179	3	10.11
CN3705	3	3
CN3720	3	3
CN3997	3	10.11
CN4175	3	2
CN7147	3	12
CN8972	3	15
UAE58	3	1
S6116	4.5	13
S6132	4.5	15
S7158	4.5	10.11
S7159b	4.5	12
S7196	4.5	12
S7209	4.5	9
S7233	4.5	15
S7249	4.5	10.11
S7251	4.5	13
S7255	4.5	8
S7433	4.5	2
S7440	4.5	15
S7461	4.5	4.5
S7462	4.5	6
CN32	4.5	4.5
CN3224	4.5	10.11
CN3709	4.5	10.11

CN5829	4.5	4.5
S7185	6	8
S7198	6	10.11
S7201b	6	6
S7203	6	6
S7216	6	7
S7231	6	6
S7259	6	12
S7507	6	7
S7570	6	7
CN3737	6	7
CN6980	6	7
CN7096	6	12
CN7112	6	6
CN7168	6	6
CN7181	6	6
CN7215	6	12
CN7960	6	6
S7264	7	7
S7486	7	15
S7510	7	4.5
S7511	7	7
S7529	7	14
S7531	7	14
S7539	7	16
S7547	7	7
S7556	7	7
S7560	7	14
CN127	7	7
CN175	7	6
CN3480	7	6
CN3491	7	6
CN3507	7	7
CN4165	7	7
CN4188	7	7
CN7212	7	6
CN7269	7	6
CN8286	7	6
S7508	8	1
S7577	8	8
S8000	8	12
CN159	8	9
CN3588	8	8
CN7971	8	8
CN8037	8	8
CN8965	8	8
S1645	9	3
S1891	9	12
S7276	9	3
S7437	9	8
S7541	9	13
S7865	9	6
S9012	9	13
S9013	9	12
CN145	9	8
CN4023	9	9
S7166	10.11	10.11
S7167b	10.11	6
S7407	10.11	6
S7415	10.11	1
S7459	10.11	4.5

S7882	10.11	6
CN4244	10.11	3
CN8298	10.11	15
UAE31	10.11	14
UAE34	10.11	9
UAE40	10.11	4.5
S6060	12	16
S7120	12	13
S7452	12	8
S7475	12	1
S7730	12	8
CN39	12	1
CN4171	12	10.11
S6102	13	13
S6123	13	13
S7526	13	13
S7533	13	13
S7551	13	12
CN3489	13	15
CN3699	13	2
CN7239	13	3
S7312	14	7
S7528	14	14
S7736	14	6
CN4174	14	2
CN7200	14	14
S6122	15	15
S7258	15	15
S7546	15	15
S7644	15	1
S7989	15	4.5
CN3717	15	13
CN8031	15	2
CN8289	15	3
CN8662	15	15
UAE44	15	3
UAE45	15	15
S7257	16	14
CN3704	16	12

Journal of Biogeography

SUPPORTING INFORMATION

Diversification in arid mountains: biogeography and cryptic diversity of the semaphore gecko *Pristurus rupestris rupestris* in Arabia

Joan Garcia-Porta, Marc Simó-Riudalbas, Michael Robinson and Salvador Carranza

Appendix S3: Supplementary figures (Figures S1–S5)

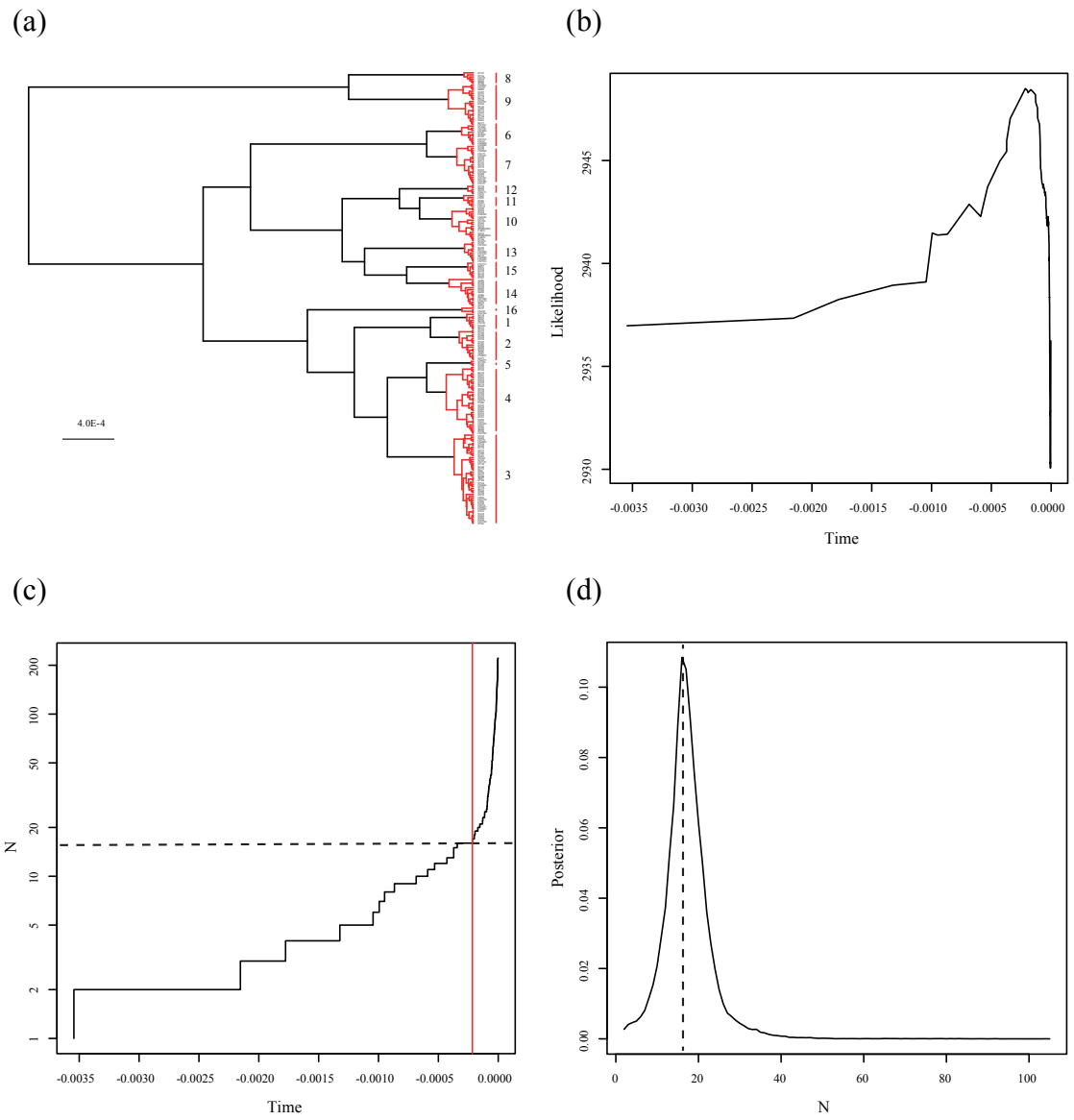

Figure S1. (a) Identification of deep mitochondrial lineages using the GMYC model to a summary tree spanning 221 unique *12S* sequences obtained from 466 specimens of *Pristurus rupestris rupestris* (dataset 1). The 16 deep mitochondrial lineages are highlighted in red and marked with their corresponding numbers (see Figure S2). (b) Likelihood surface plot and (c) lineage through time plot on which the most likely threshold separating a Yule process from a Coalescent process is placed. (d) Plot showing marginal posterior probabilities of lineage limits detected by the bGMYC approach.

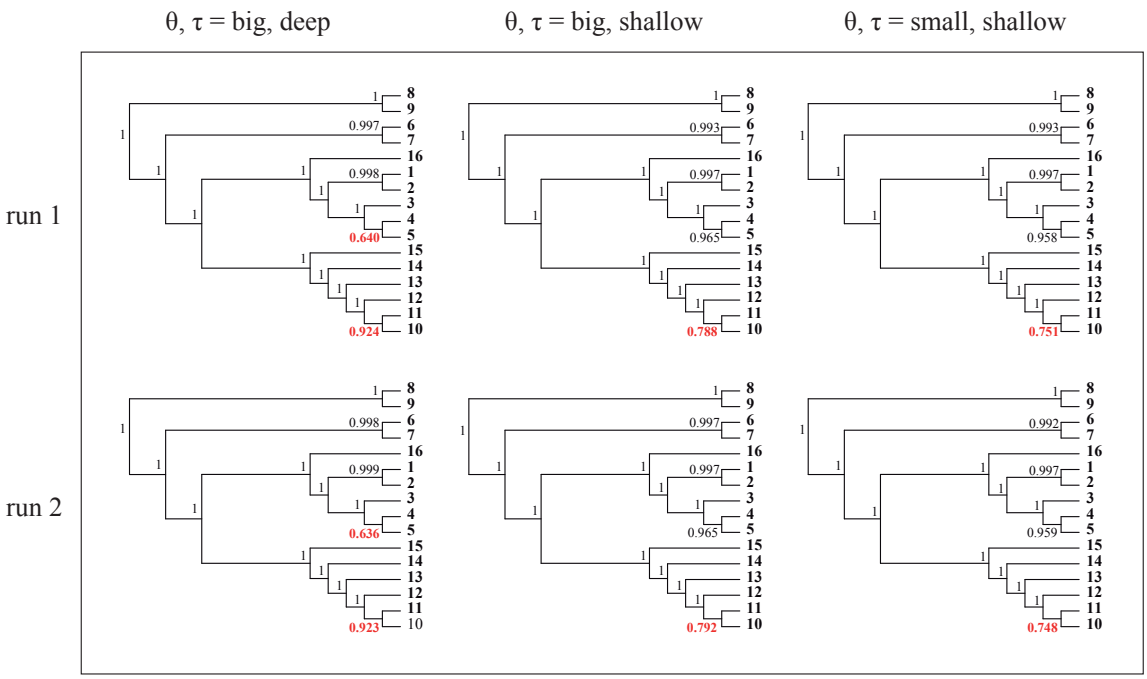

Figure S2. Chart showing the result of the species delimitation analysis of *Pristurus rupestris rupestris* inferred by BP&P (nuclear genes only) with different prior parametrizations and using as a guide tree a coalescent-based species-tree inferred with the 16 deep mitochondrial lineages detected by the GMYC/bGMYC analyses of dataset 1 (see Appendix S1 and Fig. S1). The results shown are for algorithm 0. Algorithm 1 produced almost identical results. Putative speciation events with posterior probabilities < 0.95 are highlighted in red. These were considered not reliable and its descendant tips were collapsed into the same candidate species.

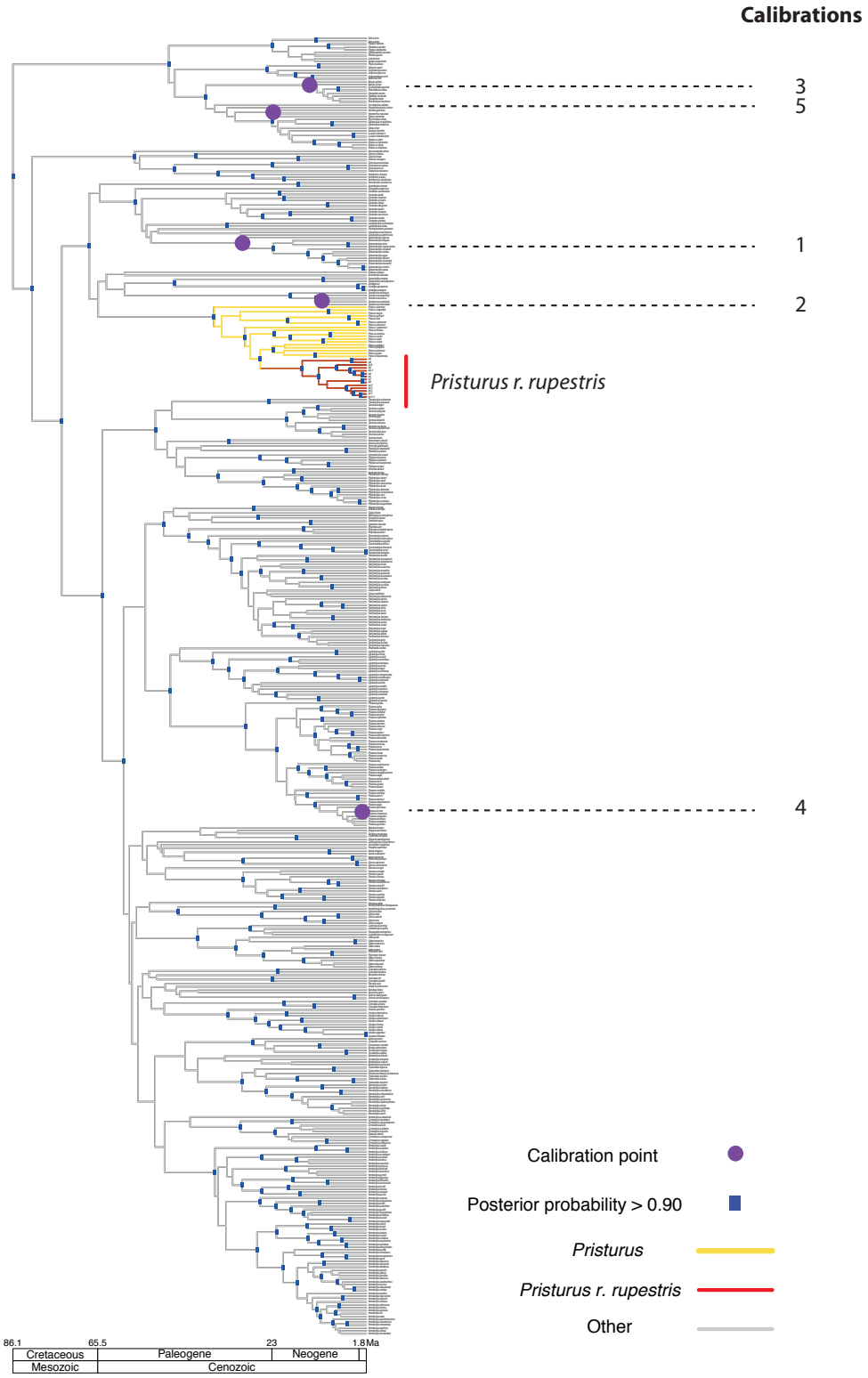

Figure S3. Time-calibrated concatenated gene tree of Gekkota inferred in BEAST with dataset 3 (two mitochondrial and three nuclear genes, 1,614 bp) including one representative of each one of the 14 candidate species of *P. rupestris rupestris* plus 435 species downloaded from GenBank, with representatives of 117 out of the 123 recognized gecko genera (see Table S2). The coloured branches refer to all 14 candidate species uncovered within *P. r. rupestris* (red) and other species in the genus *Pristurus* (yellow). The small blue rectangles highlight all nodes presenting posterior probabilities higher than 0.90. The five calibrations points used are marked with purple circles.

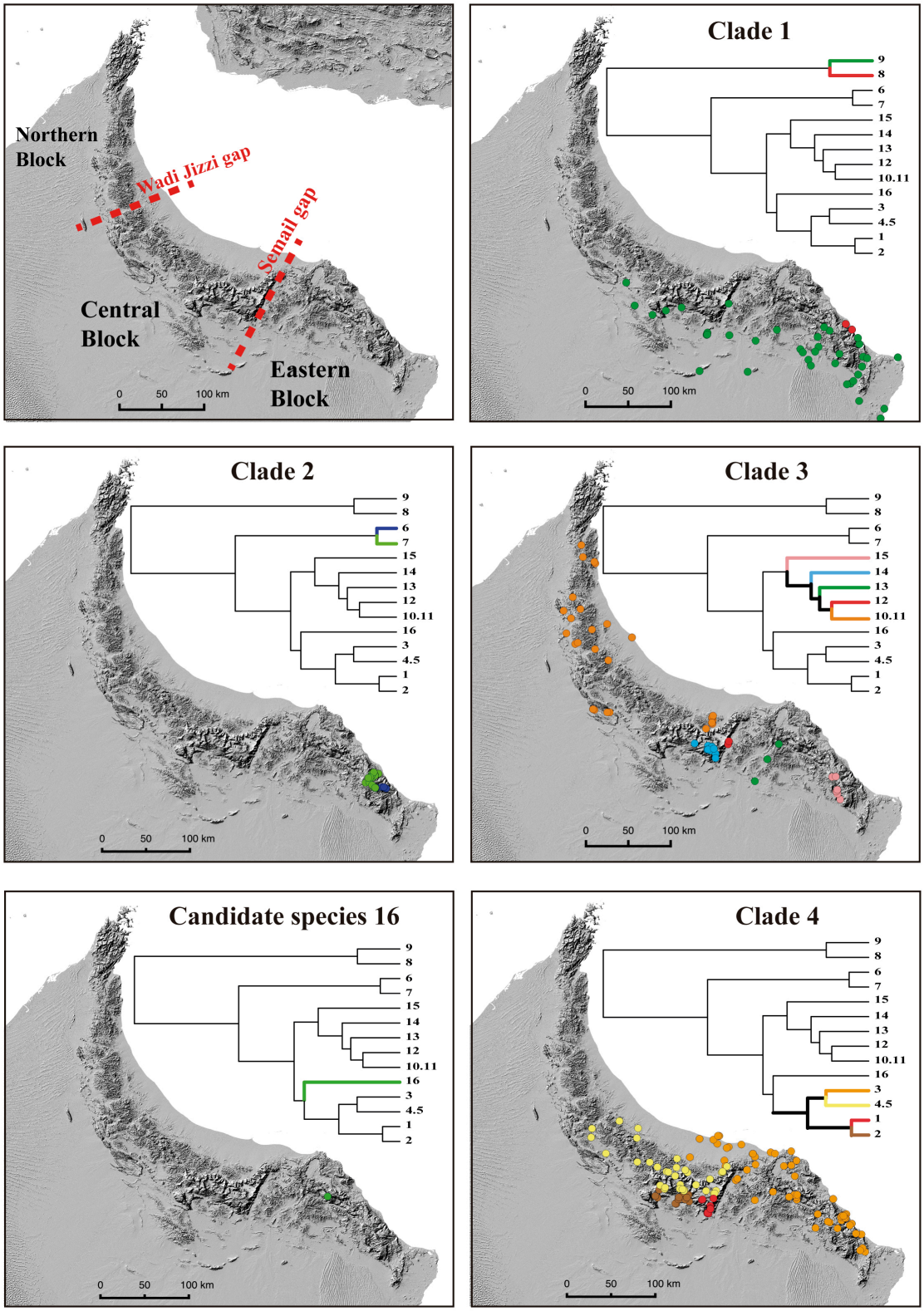

Figure S4. Distribution of the 14 candidate species of *P. rupestris rupestris* across the three discrete topographic discontinuities of the Hajar Mountains of south-eastern Arabia: the northern, central and eastern blocks, which are physically separated by the Wadi Jizzi and Semail gaps both highlighted on the first map with red dashed lines. Colours on the map correspond to the coloured branches in the species tree showed here (derived from the *BEAST analysis of dataset 2; see Fig. 2).

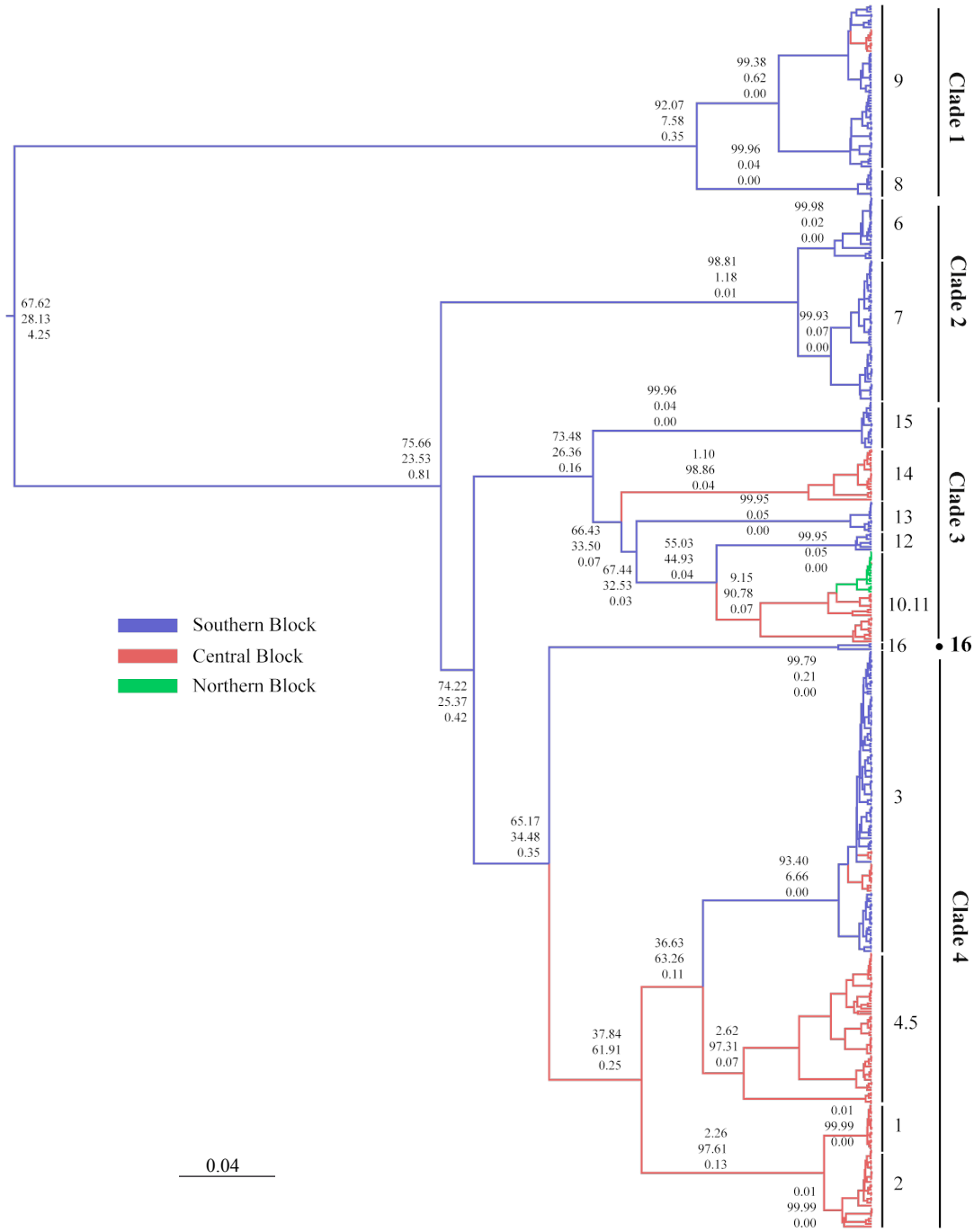

Figure S5. BEAST summary tree of the 466 specimens of *Pristurus rupestris rupestris* sequenced for the *12S* gene using the BSSVS method of ancestral area reconstruction (see Material and Methods). Branch colours indicate the inferred ancestral ranges and probability of each inferred area is presented near the major nodes (from top to bottom: southern, central and northern blocks of the Hajar Mountains of south-eastern Arabia).